Nanoscale

RSC Publishing

REVIEW

Multifunctional superparamagnetic iron oxide nanoparticles: design, synthesis and biomedical photonic applications

Cite this: *Nanoscale*, 2013, **5**, 7664

Lu Zhang,[ac] Wen-Fei Dong*[a] and Hong-Bo Sun*[ab]

Received 1st April 2013
Accepted 20th May 2013

DOI: 10.1039/c3nr01616a

www.rsc.org/nanoscale

Superparamagnetic iron oxide nanoparticles (SPIONs) have shown great promise in biomedical applications. In this review, we summarize the recent advances in the design and fabrication of core–shell and hetero-structured SPIONs and further outline some exciting developments and progresses of these multifunctional SPIONs for diagnosis, multimodality imaging, therapy, and biophotonics.

1 Introduction

SPIONs such as magnetite (Fe_3O_4) and its oxidized form maghemite (γ-Fe_2O_3) have attracted great attention in the past two decades and are being explored in biomedical applications including various separation techniques, drug delivery systems, and magnetic field-assisted radionuclide therapy.[1–5] SPIONs are biocompatible, biodegradable and potentially non-cytotoxic to humans and also show interesting properties: superparamagnetism, high saturation field, extra magnetic anisotropy contributions, irreversibility of high field magnetization, and so on.[6] Therefore, the particles no longer show magnetic interaction after the external magnetic field is removed. Owing to these unique properties, SPION-integrated multifunctional biomolecules could be tagged and detected magnetically, showing great potential to achieve *in vivo* site-targeting delivery and treatment of illnesses.[7–9] Moreover, SPIONs can also serve as magnetic resonance imaging (MRI) contrast enhancement and hyperthermia agents, immensely profiting cancer detection, diagnosis and therapy.[10–12] In addition, SPIONs open up a new avenue to the development and application of photonic technologies such as novel optical devices and non-radiotracer tomographic imaging technique in medical research.

To perform *in vivo* diagnosis, multimodality imaging and therapeutic applications, SPIONs are often coupled with other

[a]*State Key Laboratory on Integrated Optoelectronics, College of Electronic Science and Engineering, Jilin University, 2699 Qianjin Street, Changchun 130012, China. E-mail: dongwf@jlu.edu.cn; hbsun@jlu.edu.cn; Fax: +86 431-8516-8220*

[b]*College of Physics, Jilin University, 119 Jiefang Road, Changchun, 130023, China*

[c]*Max Planck Institute of Colloids and Interfaces, 14476 Am Mühlenberg 1, Potsdam, Germany*

Dr Lu Zhang received her PhD in 2011 under the supervision of Prof. Hong-Bo Sun and Prof. Wen-Fei Dong at the State Key Laboratory on Integrated Optoelectronics of Jilin University, Jilin, China. Currently, she works as a postdoctoral fellow under the guidance of Prof. Dr Helmuth Möhwald at the Department of interfaces, Max Planck Institute of Colloids and Interfaces, Potsdam, Germany. Her research interests are focused on the synthesis and application of multifunctional magnetic nanoparticles, particularly those with core–shell and hetero-structures, as well as sonochemical synthesis of novel nanostructured materials.

Dr Wen-Fei Dong received his masters in 1999 from Changchun Institute of Applied Chemistry and his PhD in 2004 from the Max-Planck-Institute of Colloids and Interfaces. From 2006 to 2008, he joined the group of Prof. Kazunori at the University of Tokyo. After that he moved to the Key Laboratory on Integrated Optoelectronics, Jilin University, as an Associate Professor. His recent research projects focus on self-assembly of biomaterials, advanced nanobiosensors and laser-based biofabrication. He has co-authored over 50 publications. In 2007, He was awarded the "Asia Excellence young researcher" from the President of the Polymer Society of Japan.

functional materials. Core/shell structure is the most common type of multifunctional SPION. This kind of nanoarchitecture is usually a magnetic core combined with fluorescent molecules, metal nanoparticles (NPs) or semiconductor nanocrystals (NCs), *etc.* These core/shell structured SPIONs with unique optical, magnetic and electrical properties have been extensively exploited, ranging from biosensing, imaging, controlled drug delivery and release, to targeting cancer therapy.[13–18] However, different components in multifunctional NPs interact with each other, which will weaken or reduce the functionality of each unit. Recent advances in nanotechnology allow the synthesis of various functional SPIONs with hetero-structure that offers a promising solution to this problem.[19,20] These anisotropic particles are currently reported as consisting of functional units with different chemistry, polarity, or other physicochemical properties on asymmetric sides without sacrificing their own properties.[21,22] The superior properties of these hetero-structured SPIONs rely on synergistically enhanced magnetism and synthesis strategies on the precise control of particle size, morphology and chemical composition. The desire to design more sophisticated nanoarchitectures with unusual properties is definitely needed.

In this review, we summarize the potentially useful design and fabrication of multifunctional SPIONs and then outline some exciting recent developments and progresses of these SPIONs in biomedical fields (Scheme 1). Finally, it is focused on the new strategies applied in innovative biophotonic applications.

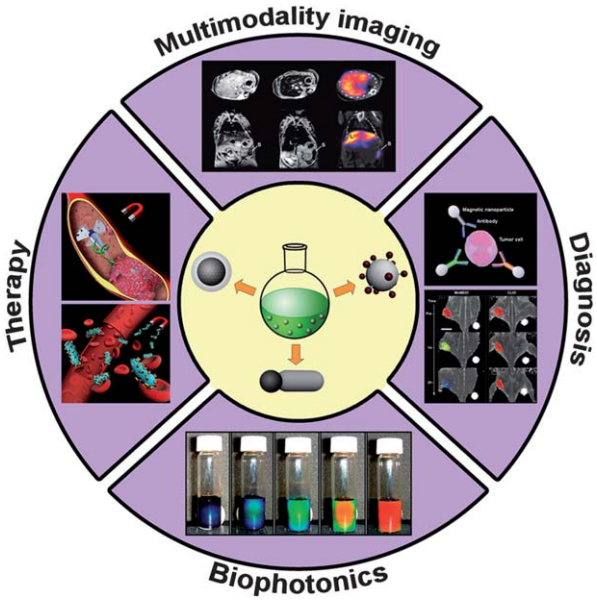

Scheme 1 Schematic diagram illustrating the applications of the three types of multifunctional SPIONs in diagnosis, multimodality imaging, therapy and biophotonics.

2 Multifunctional SPIONs

Numerous synthesis methods have been developed for the fabrication of monodisperse SPIONs in the solution phase.[23–27] General strategies are to control the nucleation and growth of NCs with a suitable capping agent and to prevent them from agglomerating—because the NPs have high surface area and aggregate easily—to minimize their surface energy. Hydrophilic SPIONs are ideal nanomaterials for biomedical applications because they can avoid being coated with plasma components and being removed from circulation rapidly.[28] However, most SPIONs with uniform size and high saturation magnetization are synthesized in an organic phase. These oleic acid- and/or oleylamine-functionalized SPIONs will be further modified with amphiphilic ligands, or the functional surfactants will be replaced by organosilanes possessing hydrophilic groups *via* a ligand exchange strategy.[29] Despite the particular advantages of intravenous injection, hydrophilic SPIONs should also be modified with a layer of hydrophilic polymer chains like derivatives of dextran and polyethylene glycol (PEG) to make them stable in the reticulo-endothelial system (RES) and possess longer circulation times. Moreover, great progress has been made in the synthesis of multifunctional SPIONs integrated by silicas,[30] plasmonic metallic NPs,[31] quantum dots (QDs),[32] rare-earth NCs,[33,34] *etc.* For this purpose, several types of iron oxide-based nanoarchitectures including core/shell,[27] Janus[35] and satellite[36,37] nanostructures have been developed. The resulting nanocomposites could exhibit unique combinations of magnetic, optical, electrical, and other properties, and have shown great potential for biomedical applications.[38]

Prof. Hong-Bo Sun received his BSc and PhD in electronics from Jilin University, China, in 1992 and 1996, respectively. In 2005, he became a full professor (Changjiang Scholar) at Jilin University, China. He won National Natural Science Funds for Distinguished Young Scholar, China, in 2005, and his team was supported by PCSIRT (Program for Changjiang Scholars and Innovative Research Team at University, China) in 2007. His research has been focused on laser micro-nanofabrication over the past 10 years, particularly in exploring novel laser technologies including direct writing and holographic lithography, as well as their applications on micro-optics, micromachines, microfluids, and microsensors.

2.1 Iron oxide NPs

Co-precipitation of Fe^{3+} and Fe^{2+} salts is a classical method employed to prepare water-soluble and biocompatible iron oxide NPs.[39,40] Iron oxide NPs can be obtained by aging a stoichiometric mixture of ferrous and ferric hydroxides in aqueous media or partially oxidized ferrous hydroxide suspensions with oxidizing agents. The size and morphology of the NPs can be controlled by adjusting the pH, reaction temperature, precursors, and the Fe(II)/Fe(III) concentration ratio. However, this

method leads to reduced control of particle shape, broad distributions of sizes and aggregation of particles. Without surface modification protection, Fe_3O_4 NPs are highly susceptible to be transformed to γ-Fe_2O_3 NPs in the presence of oxygen.[40]

High temperature decomposition is now generally used to obtain SPIONs with controlled size and morphology *via* high temperature decomposition of iron precursors in the presence of hot organic surfactants.[41–43] Metal precursors are usually metal acetylacetonates and metal oleates.[41] Oleic acid and oleylamine act as stabilizers and reducing agents. The size and shape of iron oxide NPs could be controlled by adjusting the reaction temperature and the molar ratio of precursor to stabilizer. This approach is a common method to synthesize various iron oxides, including Fe_3O_4, γ-Fe_2O_3 and hematite (α-Fe_2O_3) NPs.[44]

High temperature decomposition usually requires a complicated process and high temperature. As an alternative, hydrothermal synthesis has received extensive attention. This approach includes various technologies for crystallizing a substance in a sealed container from a high temperature aqueous solution at high vapor pressure, which is prone to well-crystallized magnetic NPs with high saturation magnetization.[45,46] Moreover, hydrothermal treatment is able to fabricate unusual iron oxide NP-like nanocubes and hollow spheres.[47,48]

Recently, the solvothermal synthesis method has been extensively studied for fabricating novel magnetic nanoclusters.[49,50] Ge *et al.* synthesized highly water-dispersed superparamagnetic nanoclusters using a one-pot high-temperature hydrolysis and reduction of iron chloride hydrate in ethylene glycol with poly(acrylic acid) (PAA) as surfactant.[51] Each cluster with the size of 30–180 nm is composed of many magnetite crystallites of approximately 10 nm, thus retaining the superparamagnetic property at room temperature. Zhao *et al.* fabricated sodium citrate-stabilized magnetic clusters to improve biocompatibility with the aim of targeted drug delivery using the same solvothermal approach.[52] The strategy of forming clusters of magnetite NCs not only avoids the superparamagnetic–ferromagnetic transition but also increases the magnetization of the magnetic NPs.

Sonochemical method as a "clean and green" alternative method has attracted significant attention.[53,54] Sonochemistry arises from acoustic cavitation: the formation, growth and implosive collapse of bubbles in a liquid. The implosive collapse of the bubbles produces extremely increased pressures, temperatures, and heating and cooling rates.[55] These extreme conditions promote the formation of the new phase and increase the mass transfer rates, which lead to the preparation and design of novel materials with unusual properties. The versatility has been successfully demonstrated in the fabrication of various iron oxide materials.[56]

2.2 Core/shell NPs

Monofunctional magnetic NPs cannot meet the needs of growing demands from medical and other fields. In the past two decades, attention have been paid to the fabrication of multifunctional SPIONs. To integrate functional materials into one entity, various common chemistry concepts have been applied in the design and synthesis of core/shell structured SPIONs. Magnetic silica core–shell NPs have been extensively studied since the silica surface allows for additional functionalization and improves the chemical stability of the composites. The general approach is based on the well-known Stöber process, which comprises the hydrolysis and polycondensation of tetraethoxysilane under alkaline conditions in ethanol.[57,58] Fig. 1 shows the TEM images of 12.2 nm Fe_3O_4@SiO_2 NPs coated with different silica shell thicknesses by simply changing the TEOS amounts. By employing a sol–gel method, fluorescent dyes could be further incorporated into the SiO_2 shell to obtain a magnetic-luminescent nanocomposite, which can be observed and manipulated with fluorescence microscopy and an externally applied magnetic field, respectively.[59] As most organic dyes suffer from severe photobleaching during the detection process,[60] in recent years, semiconductor QDs as good alternatives to fluorescent dyes have been applied in *in vivo* imaging because of their photostability.[61] Wang *et al.* first described the formation of magnetic-luminescent NPs that consist of a polymer coated γ-Fe_2O_3 superparamagnetic core and a CdSe/ZnS QDs shell.[62] The general strategies for the deposition of QDs on the Fe_3O_4 magnetic NPs are the covalent coupling of various ligands to the particle surface and layer-by-layer self-assembly approach.[63]

Compared with visible light excitation, near-infrared (NIR) light excitation has been considered as a new generation of optical imaging technique for *in vivo* imaging for the advantages of deep penetration, weak autofluorescence, minimal photobleaching and low phototoxicity.[64–67] Rare-earth upconversion NCs are the most prominent luminescent probes for *in vivo* imaging. Early synthetic prototypes of magnetic/upconversion core/shell nanocomposites employed SiO_2 as a protective coating in the middle layer. Recently, more and more work has been focused on non-silica core/shell NCs. These novel nanocomposites exhibit excellent superparamagnetic properties and T_2-enhanced MR effect and can emit visible light at 980 nm

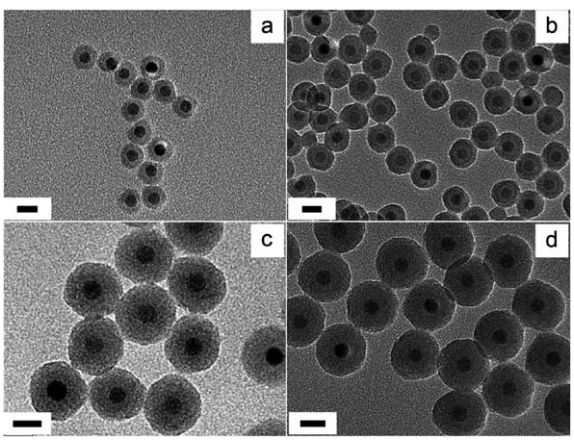

Fig. 1 TEM images of 12.2 nm Fe_3O_4@SiO_2 NPs with different TEOS amounts: (a) 75, (b) 150, (c) 300 and (d) 600 μL. Scale bar = 20 nm. Reprinted from ref. 58 with permission from the American Chemical Society.

excitation. Li's group have done a series of studies on developing multifunctional upconversion NCs for bioimaging of small animals.[68] A facile homogenous co-precipitation method was recently developed to synthesize core/shell Fe_3O_4@LaF_3:Yb,Er mesoparticles.[69]

Another promising core/shell nanocomposite is the magnetic/metallic nanostructure. Gold and silver are the most abundantly used metals due to their outstanding optical properties such as localized surface plasmon resonance. Analyte molecules can be easily captured and magnetically concentrated by magnetic/metallic NPs and can further be analyzed by surface enhanced Raman scattering (SERS). For instance, magnetic core/shell Fe_3O_4/Au NPs with tunable plasmonic property were synthesized.[70] Xu *et al.* employ low-temperature coating of Au on the surface of Fe_3O_4 NPs by reducing $HAuCl_4$ in a chloroform solution of oleylamine. The resulting NPs serve as seeds for the formation of Fe_3O_4/Au NPs with thicker Au coatings achieved by adding more $HAuCl_4$ under reductive conditions. Superparamagnetic Fe_3O_4/Ag core/shell nanocomposites were also fabricated by a simple one-pot thermal decomposition method, which could serve as an antibacterial agent.[71] To reduce the interference of two individual components, an inert silica shell is usually introduced in the general design of a core–shell structure. Fe_3O_4 NP was first coated with a uniform shell of amorphous silica to keep individual magnetic NPs apart, and then a gold shell was coated on the surface of silica by a simple seed-mediated method.[72] These unique core/shell SPIONs are promising multimodality probes for *in vivo* imaging.

2.3 Hetero-NPs

2.3.1 Magnetic Janus NPs. Magnetic Janus NPs, which consist of iron oxide with materials of different physicochemical properties on opposite sides, have emerged as a new division of multifunctional SPIONs.[73] These anisotropic/asymmetric particles are mainly synthesized by sequential growth of a second component on pre-formed magnetic seeds. The nucleation and growth is anisotropically anchored onto one specific crystal plane of the seed. Such a growth pattern will reduce the contact of the combined individual components in contrast with a core/shell structure,[74] so that their fingerprint optical, magnetic, and electronic properties are not often interfered with or completely lost.[75,76] Therefore, the unique structure gives SPIONs great potential in drug delivery, imaging probes and electronic devices.[77,78]

The most studied magnetic Janus particles are magnetic-noble metal ones. Sun's group first fabricated Fe_3O_4–Au Janus particles *via* the decomposition of iron pentacarbonyl ($Fe(CO)_5$) on the surface of gold NPs, followed by oxidation in air.[79] The size of Fe_3O_4 NPs could be controlled by adjusting the $Fe(CO)_5$/Au ratio. The mechanism of controlled nucleation and growth is attributed to the possible electron transfer between Au and Fe. This method was also exploited in preparing other Janus-like (Fe_3O_4–Pt, Pd, Ag) NPs.[80] Gu's group synthesized Fe_3O_4–Ag Janus NPs by ultrasonication of a heterogeneous solution of as-prepared Fe_3O_4 NPs in an organic solution and $AgNO_3$ in water.[81] The reaction takes place on the exposed surface of the NPs which assembled at a liquid–liquid interface to form a capsule. In addition, a hollow iron oxide–silver NP has also been fabricated based on the reaction at the liquid–liquid interface.[82] In a two phase mixture of hexane and water of silver nitrate, iron oxide NPs can form a colloidosome at the two phase interface and catalyze the reduction of silver ions to obtain a hollow heterodimer nanostructure. This work provides an effective approach for fabricating a multifunctional nanostructure.

Another promising magnetic Janus NP is a magnetic-silica heterostructure. Gao's group developed a flame synthetic route to obtain a novel spherical Janus particle consisting of γ-Fe_2O_3 and SiO_2 bicompartments upon ignition of the methanol solution of ferric triacetylacetonate ($Fe(acac)_3$) and tetraethyl orthosilicate (TEOS).[83] Feyen *et al.* produced a Janus-like Fe_3O_4–polymer–SiO_2 NP through partial encapsulation of an iron oxide NP in a polymer nanosphere and spatially controlled anchoring of SiO_2 with Fe_3O_4 NP as the nucleation site *via* a modified Stöber process.[86] The excellent structural properties of these particles enable further modification. Soon after, Zhang *et al.* reported a modified sol–gel process for the fabrication of a Janus particle with a magnetic Fe_3O_4 head and a mesoporous SiO_2 body. Such nanocomposites have superior magnetic properties, well-defined pore structures, and uniform size with controlled aspect-ratio (Fig. 2).[84] These Janus NPs could easily self-assemble at the liquid–liquid interface without any surfactant, displaying the well assembled properties of such a heterostructure.[85]

Magnetic-QD Janus NPs were also studied as a novel luminescent imaging nanoprobe. The sequential growth of CdS onto the γ-Fe_2O_3 NPs was formed by the direct addition of sulfur and metal reagents to the γ-Fe_2O_3 NP reaction mixture at a higher reaction temperature, which endows them with both attractive fluorescent and magnetoresponsive capabilities.[87,88] A microfluidic synthesis method was also employed to fabricate Janus superballs with distinct magnetic-NPs and quantum dots on

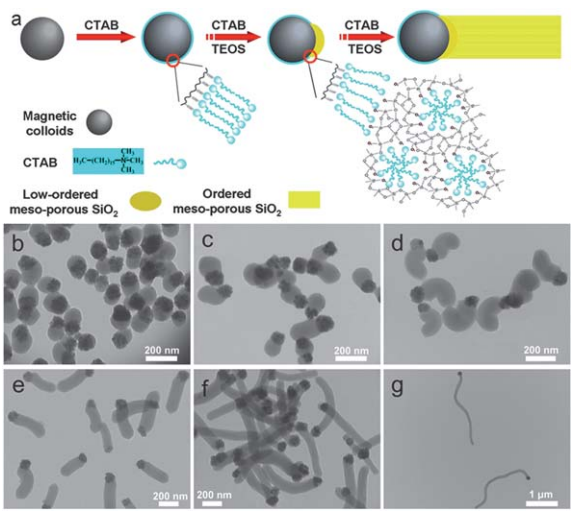

Fig. 2 (a) Strategy used to grow a mesoporous silica stick on a Fe_3O_4 NP. TEM images of Fe_3O_4–SiO_2 Janus particles with different aspect ratios of 2 : 1 (b), 3 : 1 (c), 4 : 1 (d) 5 : 1 (e), 7 : 1 (f), and a μm-long worm-like Janus particle (g). Reproduced from ref. 84.

opposite sites,[89] which could be further used as a magneto-driven fluorescent switch for free-writing under a magnet.

2.3.2 Core–satellite NPs. Core–satellite NPs, another interesting model of multifunctional SPIONs, possess one single core with the attachment of various smaller particles through electrostatic interactions or covalent bonds. The most common core–satellite particle is Fe_3O_4–noble metal nanocomposite.[90,91] Usually this kind particle is thought to be the intermediate for the conversion to core/shell NPs. However, core–satellite NPs have an uncovered core surface eligible for further functionalization and a high surface area of satellite material for specific functions. Moreover, this structure can reduce the interference of two individual components. Generally, γ-Fe_2O_3 or Fe_3O_4 NPs could be coated with organic polymers or lysine and subjected to the attachment of anionic gold NPs. Fe_3O_4/polymer/Au and γ-Fe_2O_3/lysine/Au core/satellite nanocomposites were easily obtained.[93,94] Moreover, iron oxide NPs could be first coated with uniform silica shells *via* sol–gel reaction followed by aminosilanization. Then, negatively charged citrate-coated gold NPs could be attached onto the positively charged Fe_2O_3/SiO_2 NPs *via* electrostatic interactions, yielding the core/shell–satellite nanocomposites.[92,95] Accordingly, a core–satellite Fe_3O_4–Pd heterostructure could also be obtained by generating Pd NPs at the pluronic polymer-coated surface of Fe_3O_4. It has been demonstrated that these core–satellite structured Fe_3O_4–Pd nanocomposites have higher catalytic activity than the core/shell ones.[96]

Recently two types of core/satellite magnetic-luminescent nanocomposites have been developed. The first kind is fluorescent molecular-doped silica core and multiple satellites of magnetic NPs. This core–satellite nanostructure possesses high photostability because of dye molecules protected by a silica matrix, which is beneficial for the cultivation of multiple magnetic NPs onto a single nanoprobe as shown in Fig. 3.[97] As-formed nanocomposites have superior MRI and fluorescence capabilities with four-fold improvement. They were confirmed as excellent dual-imaging probes for the detection of polysialic acids expressed on various cell lines. Another magnetic-luminescent nanocomposite has a magnetic core and multiple satellites of dye molecules or QDs. For instance, hydroxylated Fe_3O_4 NPs have been linked to the *N*-hydroxysuccinimide esters of the Cy5.5 dye by means of intermediate functionalization with amino-polyethylene glycol (PEG)–silane molecules. The PEG molecules were first linked to the NPs surface through silanol groups and then their terminal primary amines were reacted with NHS-Cy5.5 molecules.[98] Another example is that of a SPION core decorated with satellite CdS:Mn/ZnS QDs by a heterobifunctional cross-linker molecule, which carried the cancer-fighting agent signal transducer and activator of transcription 3 (STAT3) inhibitor.[99] In addition, a polyelectrolyte intermediate layer was usually introduced to separate the magnetic core and the satellite ODs. An example is that negatively charged thioglycolic acid-capped CdTe NPs were attached to the positively charged polyallylamine shell of the magnetic NPs.[100] Such multifunctional hetero-NPs could serve as a platform technology for the next-generation of probes for detection and imaging.

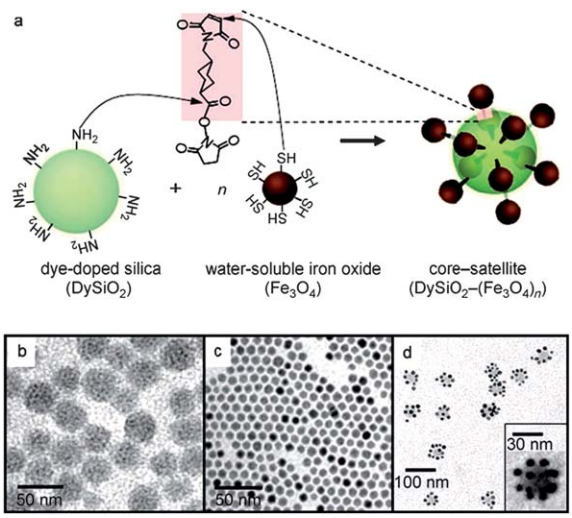

Fig. 3 (a) Schematic diagram for the synthesis of core–satellite $DySiO_2$–$(Fe_3O_4)_n$ NPs. (b–d) TEM images of (b) rhodaminedoped silica ($DySiO_2$), (c) Fe_3O_4, and (d) core–satellite $DySiO_2$–$(Fe_3O_4)_n$ NPs. Reprinted from ref. 97 with permission from John Wiley and Sons.

3 SPIONs in diagnosis

The rapid, sensitive, and high-throughput detection of potential disease biomarkers is critical for the early diagnosis and treatment of disease. In this regard, magnetic NPs have been used due to their unique magnetic properties allowing for efficient target capture, enrichment and convenient separation. The utilization of these biofunctional magnetic NPs for binding target molecules can result in the effective separation of nucleic acids, proteins, viruses, bacteria and cells, which is beneficial for signal amplification and readout strategies. Over the past few years, the application of SPIONs for early clinical diagnostics has been extensively reported.[101,102] This section will highlight some of the most recent developments of SPION-based ultrasensitive assays as the basis of several tests.

3.1 DNA molecule detection

Genomic DNA detection such as nucleic acid hybridization, polymerase chain reaction (PCR), and microarray technologies are reliable methods for the diagnosis of genetic and pathogenic diseases.[103] These detection techniques mainly use oligo- or polynucleotide probes containing covalently linked reporter groups (radioactive labels, fluorescent labels, *etc.*) to target a polynucleotide *via* hybridization that distinguishes one individual's genome from another's and can provide clues to pathogenetic disease.[104] Although these methods are well-studied, the emergence of nanotechnology in the past few decades has now enabled the improvement of the sensitivity and accuracy of DNA diagnostic systems. In particular, magnetic NP-based assays have proven to be extremely effective in biomedical research.[105]

An early attempt was made by Jungell-Nortamo's group using oligonucleotide-functionalized magnetic microbeads for

isolation of specific nucleic acid sequences.[106] The capture DNA is coupled to the polystyrene-hydroxy surface of magnetic microbeads through *p*-toluenesulfonyl chloride activation. This method offers simplicity and convenience to collect the formed hybrids, and increases the reaction rate compared to filter-based DNA hybridization. Recently, the magnetic particle-based assay has also been applied in the extraction of DNA from viruses and bacteria. To further facilitate the adaptation of this method, a novel class of DNA detection method that integrated other technologies in one system was developed with the goal of increasing the specificity and efficiency of probes. For example, Parham *et al.* employed a specific magnetic bead-based probe for the capture of the genomic DNA (gDNA) of Group B streptococci (GBS), a leading cause of sepsis and meningitis in newborns.[107] The modified SPIONs with target nucleic acids of different lengths can efficiently capture GBS gDNA from both bacterial cultures and vaginal/anal samples. This technology combines sample preparation with detection technologies to allow point-of-care testing and its efficiency of gDNA capture increases with oligonucleotide length. Additionally, Xi *et al.* developed a gold-coated iron oxide NP gene probe for the detection of Hepatitis B virus (HBV) DNA.[108] Iron oxide–gold NPs were prepared by the citrate reduction of tetra-chloroauric acid in the presence of iron oxide NPs which were added as seeds, and then were modified by hexanethiol 30-mer oligonucleotides. HBV DNA could target at the magnetic NP surface and be concentrated from diverse organic samples and purified. The detection of HBV DNA could be directly observed by TEM and blot hybridization.

3.2 Protein detection

Proteins are another important group of biomarkers that can provide a "snapshot" of patient status by detecting and monitoring their levels for clinical analysis.[109] Currently, the related assay in clinical disease diagnosis mainly uses the enzyme-linked immunosorbent assay (ELISA).[110] It needs a surface immobilized antibody1 (Ab1) and an enzyme-linked Ab2 to sandwich the target for sensitive enzymatic detection. This means that the ELISA method can only be used to analyze one or a few samples at a time and is not suitable for high-throughput assays with reduced assay volumes. In recent years, magnetic NPs have attracted significant research interests for multiplex protein analysis due to their advantages over the standard method, such as sensitivity, high surface area, easy modification/operation, low sample requirements, and assay miniaturization. Thus, SPION-based ultrasensitive biosensors are now becoming one of the most powerful tools for protein detection.[111] Like the ELISA method, antibodies are still mostly used for the recognition and capture of proteins, but SPIONs have larger surface areas where more capture biomolecules can be immobilized to detect a wide range of target proteins. Furthermore, magnetic NPs aggregate under the induction of a magnetic field for sensitive molecular detection and can be integrated into several micro-devices (*e.g.*: transducer devices, microfluidic devices, electronic devices) to detect trace amounts of proteins in an automatic manner. Up to now, a variety of new design strategies on how to use magnetic NPs for protein detection have been successfully reported. Mirkin's group utilized an Ab-conjugated magnetic microparticle (Ab1-MMP) tagged with barcode DNAs (Ab2-GNP), which were used to sandwich prostate-specific antigen (PSA), a protein biomarker for prostate cancer (Fig. 4).[112] The formed sandwich MMP-Ab1/PSA/Ab2-GNP composite was separated and washed by a magnetic field. Then the released barcode DNAs from the sandwich convert PSA into hundreds of barcode DNAs, which were detected sensitively by scanometric assay coupled with silver amplification. This method integrates efficient target capture, enrichment, conversion and amplification, showing its great potential in early clinical diagnosis. Perez *et al.* prepared avidin–P1 conjugates as generic reagents for the attachment of any biotinylated antibody.[113] Biotinylated anti-green fluorescent protein (GFP) polyclonal antibody was then attached to yield an anti-GFP-P1 nanosensor. When the nanosensors were used to detect for GFP protein, significant changes in the T_2 relaxation time were observed. These changes were time and dose dependent. This assay avoids the substances interacting with light and does not require a wash step to remove unbound analytes. It could also be used to sense enzymatic activity.

In addition, novel portable protein test systems have been developed for both basic research and clinical practice. For example, Weissleder's group developed a miniaturized, micro-nuclear magnetic resonance (μNMR) system for rapid protein analysis based on NMR technique.[114–116] When antibody-attached magnetic NPs bind to their protein targets through affinity ligands, they form soluble nanoclusters, which lead to the shortening of the T_2 relaxation time of surrounding water molecules. This assay method could enable the detection of a variety of targets in microliter sample volumes. Recently, Wang's group developed a magnetically responsive giant magnetoresistive (GMR) nanosensor for protein detection.[117–119] The GMR nanosensor, consisting of a spin valve sensor array and magnetic NPs, can sensitively and quantitatively recognize multiple protein tumor markers in mouse and human serum samples. This technology allows the rapid conversion of discrete interaction events among biomolecules into electrical signals in real time.

Besides antibodies, other molecules can also be bioconjugated with SPIONs. For instance, SPIONs could be functionalized with aptamer combining MRI technology for the detection of human α-thrombin protein.[120] The contrast effect is due to the assembly of the aptamer functionalized SPIONs in the presence of thrombin. A change in the MRI signal was detected even at a trace concentration of thrombin in human serum. This system was specific to thrombin because the changes of MRI signal were not observed with other analytes like bovine serum albumin and streptavidin. Yan *et al.* developed a simple method for the immobilization of unmodified monosaccharides (MSs) onto SPION surfaces,[121] where MSs were used as targeting ligands for sensing proteins. MSs were covalent coupled onto the SPION surface resulting in glyco-NPs by using CH insertion reaction of photochemically activated phosphate-functionalized perfluorophenylazides. The surface-bound MSs possess a mannose-specific receptor and recognition ability for concanavalin A.

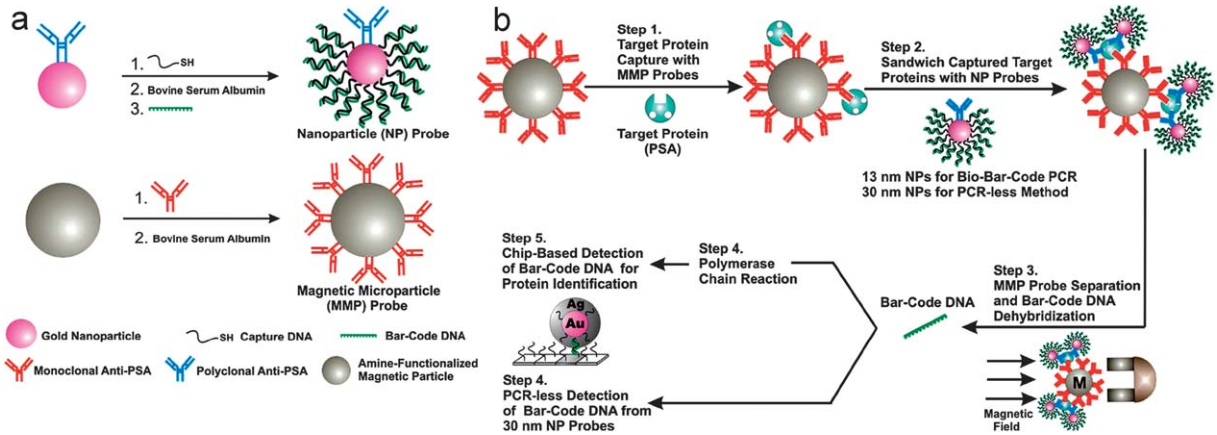

Fig. 4 The biobarcode assay method. (a) Probe design and preparation. (b) PSA detection, barcode DNA amplification and identification. The number of bound NP probes for each PSA is unknown and will depend upon target protein concentration. Reprinted from ref. 112 with permission from the American Association for the Advancement of Science.

These studies imply that MP-based sensitive biosensors have great potential in clinical diagnosis.

3.3 Virus detection

A virus is a small infectious agent that can infect human beings and cause a serious health problem.[122] Early stage detection in patients is very important because accurate diagnosis of a virus could not only enhance recovery but also limit the rapid spread of the infectious disease. Thus, a rapid, sensitive, and specific detection method that is capable of simultaneously identifying multiple pathogens in complex samples is urgently needed.[123]

The conventional virological approaches for the detection and analysis of influenza virus (influenza antigens or enzymes) are viral isolation culture with immunocytological confirmation and hemagglutination-inhibition (HI).[124] These methods offer high sensitivity and specificity but require several hours to days for the culture and detection. The recent development of SPIONs has made it possible to rapidly and efficiently separate the interested virus type from complex mixtures and concentrate it for ultrasensitive detection. This technique uses SPIONs coated with receptor molecules that interact with viruses according to their unique surface features (*e.g.*: charge and specific antigens) and then separates the target virus from the sample by applying a magnet field and washing. Taking a highly positively charged virus for example, Sakudo *et al.* developed an anionic polymer, poly(methyl vinyl ether–maleic anhydride) (PMV/MA) coated magnetic beads for facilitating the detection of borna disease virus (BDV), a noncytolytic, neurotrophic virus that could infect all warm-blooded animals and possibly humans.[125] As-formed composites can succeed in the capture and concentration of BDV by electrostatic interactions. In the captured BDV, the presence of a viral genome, N protein, and P protein was confirmed by RT-PCR and Western blotting. This method facilitates the isolation of infectious BDV from tissues and body fluid and could also combine with other conventional detection methods for the analysis and prevention of BDV infectious diseases. In addition, Kamikawa *et al.* developed an aniline monomer polymerized on γ-Fe_2O_3 to obtain a SPION–polyaniline biosensor architecture that can serve as a charge transfer biosensor for direct detection of a surface glycoprotein hemagglutinin (HA) from the Influenza A virus (FLUAV) H5N1.[126] SPION–polyaniline probe was functionalized with α-H5 monoclonal antibody or α-H1 polyclonal antibody against target HA. Researchers have found that the anti-HA-SPIONs–polyaniline complexes were able to immunomagnetically separate target HA from the serum matrix, which demonstrates that the novel design can serve as the biosensor probe for cyclic voltammetry (CV) assay in disease monitoring and biosecurity.

3.4 Bacterial detection

Bacterial infection or contamination associated with disease control, environmental monitoring and food safety is also a major issue in public health.[127] To date, considerable progress has been achieved for MP-based biosensors by coupling sensitive biosensors with magnetic separation to detect pathogenic bacteria for addressing the analytical needs of medical diagnostic systems.[128,129] This method generally involves two steps. The first is target capture, in which three classes of capture methods such as surface recognition method, nucleic acid method mentioned in DNA detection, and protein–ligand method are used. The second step is to quantify the captured, tagged or amplified material using optical, electrochemical or piezoelectric technologies.

Surface recognition method, including immunoassay technique and molecule-specific probe, is the most widely used bacterial detection approach, which captures target bacteria by binding to molecular structures on their exterior surface or to structures within their interior space. Using this method, Grossman *et al.* have employed SPIONs for rapid detection of magnetically labeled *L. monocytogenes*.[130] SPIONs of 50 nm size were first coated with antibodies. Then SPION–Ab was dispersed into an aqueous solution containing *L. monocytogenes* and the internal magnetic dipole moments of these particles were aligned under a pulsed magnetic field. Particles bound to

L. monocytogenes were fixed and could relax in about 1 s by rotation of the dipole moment. This magnetic relaxation signal was generated after the turn-off of the magnetic field and could be measured using a high-transition temperature superconducting quantum interference device. Similarly, small molecules like carbohydrate can be immobilized on SPION surfaces for the detection of bacteria. For instance, silica coated magnetite NPs functionalized with carbohydrate D-mannose were studied for the detection of bacteria *E. coli*.[131] The carbohydrate provides an anchor to the bacteria for attachment to the mammalian cell which subsequently results in the infection. The carbohydrate coated SPIONs could detect *E. coli* with a total assay time of less than 5 min. About 88% of the bacteria can be removed from the media by magnetic separation due to the high surface are of the MGNPs. This method could be used for distinguishing pathogen strains in clinical diagnosis.

Furthermore, Koets *et al.* have developed a powerful and specific biosensor using SPIONs as detection labels for *E. coli* and *Salmonella*. Genomic bacterial DNA was used as a template for polymerase chain reaction (PCR) using a 50-biotin forward primer and a 50-fluorescein reverse primer.[132] The double-stranded-PCR product was then mixed with streptavidin-coated SPIONs. Finally, the particle complexes were captured by anti-fluorescein antibodies and detected with the GMR sensor device. This SPION-based biosensor has high sensitivity, so that a trace concentration of amplicon (4–250 pM) was detected by a one-step approach with an assay time in 3 min.

Virus particles could also be conjugated to SPIONs for detecting *S. aureus* bacteria. Douglas' group demonstrated that cowpea chlorotic mottle virus (CCMV) was labeled with fluorescent and MRI contrast agents and then targeted to a biofilm of *S. aureus*.[133] The targeting strategy was based on protein–ligand interaction that consisted of streptavidin sandwiched between biotinylated CCMV and biotinylated anti-protein A monoclonal antibody. The antibody was bound to the protein A that is expressed on the bacterial cell surface. The successive targeting of CCMV with *S. aureus* could be simply confirmed by flow cytometry analysis and epi-fluorescence microscopy.

3.5 Cell detection

Magnetic NP-based biosensors have become increasingly used in the field of cell detection, especially for the development of novel approaches to detect tumor cells in early stages for diagnostic or prognostic purposes, as shown in Fig. 5.[134–137] The surface-modified magnetic NPs can bind to a variety of specific cell receptors for the detection of a desired cell from a complex cell population, allowing them to sensitively accumulate in the tumor cells for patient assessment and management by other imaging techniques.

Choi *et al.* first reported the *in vivo* study with dextran-coated SPIONs of 26 nm size functionalized with folate ligands for specific detection of nasopharyngeal epidermal carcinoma (NPEC) cells.[138] The uptake of tumor cells by folate–SPIONs could reduce the tumor signal intensity by 38% on T_2-weighted MRI result. Later, Chen *et al.* used folate-conjugated SPIONs coated in PEG instead of dextran for performing *in vivo* studies

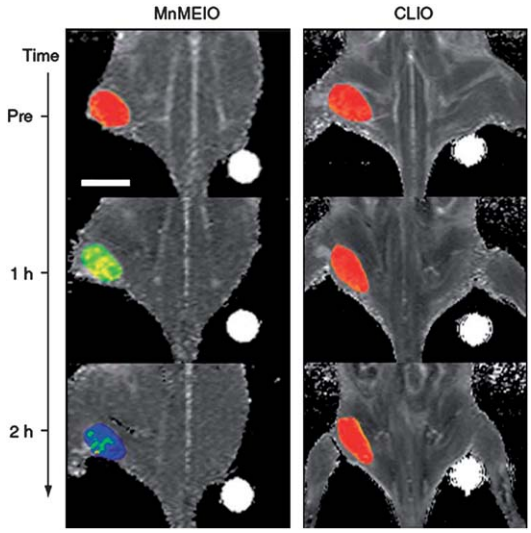

Fig. 5 Color maps of T_2-weighted MR images of a mouse implanted with the cancer cell line NIH3T6.7, at different time points after injection of magnetic NP–herceptin conjugates or CLIO–Herceptin conjugates. In the first row, gradual color changes at the tumor site, from red (low R_2) to blue (high R_2), indicate progressive targeting by MnMEIO–Herceptin conjugates. In contrast, almost no change was seen in the mouse treated with CLIO–Herceptin conjugates. Reprinted from ref. 134 with permission from Nature Publishing Group.

for NPEC cells detection.[139] They found that the particles reduced the tumor signal on T_2-weighted images by 20–25%. The decrease in tumor signal intensity demonstrated that MRI or CT could easily determine the difference between tumor and healthy tissues. The folate ligands could facilitate selective uptake of SPIONs into cancerous tissues. Cyclic Arg-Gly-Asp (cRGD) peptide has been coupled to SPIONs with various sizes for *in vivo* studies with human umbilical vein endothelial cells. cRGD-conjugated SPIONs showed a strong specific uptake of the cancer cell lines attributed to the uptake of the particles by integrin-expressing cells.[140]

Ab–SPION conjugates were used for the uptake of cancer cell for *in vivo* diagnostics. Compared to the untargeted control SPIONs, Ab–SPION conjugates showed a significant accumulation of the conjugated particles in a mouse model of colorectal carcinoma cells.[141] The real-time observation of esophageal squamous cell carcinoma cells by transmission electron microscopy (TEM) showed that anti-epidermal growth factor receptor antibody-conjugated SPIONs had been internalized by the cancer cells and were residing in lysosomes after SPION injection.[142] This study demonstrates the ability of antibodies to act as effective targeting ligands for SPIONs, leading to a strong specificity for antigen-expressing tissues and effective contrast enhancement.

Aptamers were also conjugated to the surfaces of SPIONs through various methods for diagnostic applications. SPION–aptamer conjugates have been used to magnetically separate specific blood cancer cell lines from complex mixtures including whole blood and serum.[143,144] Yigit *et al.* developed a novel aptamer–SPION for the detection of adenosine in biological samples, which demonstrated aptamer–SPION probes owning a high degree of specificity and affinity for their targets.[145] These studies serve as a convincing "proof of

concept" to demonstrate these versatile ligands as highly selective and to identify targeting ligands to a nearly limitless variety of cancers for future clinical applications.

4 SPIONs in multimodality imaging

Molecular imaging technology allowing the display and quantification of biological processes at the cellular and molecular levels has been an important tool for the diagnosis and treatment of diseases in their earliest stages. Classic imaging techniques, such as MRI, optical imaging, computed tomography (CT), ultrasonography (US) and positron emission tomography (PET), have shown great promise in the clinical arena. In recent years, SPIONs as contrast agents have been successfully used in MRI, which is a well-known medical imaging technique to visualize internal structures of the body in detail based on NMR. The signal of the magnetic moment of a proton around magnetic NPs can be captured by resonant absorption. SPIONs can reduce the T_2 relaxation time of tissue water due to the spin interaction between electron spins of SPION and water proton, showing a darker MR imaging. MRI has been considered as one of the most powerful clinical diagnostic techniques for the evaluation of various diseases, especially for liver imaging due to its high spatial and contrast resolution and low ionizing radiation. However, a single technique does not possess all the required capabilities for comprehensive imaging. Thus, multimodal medical imaging is becoming a research focus for state-of-the-art biomedical research because it can provide complementary information from each imaging technique. In this section, an overview of MRI-guided multimodality is presented.

4.1 MR/CT imaging

CT is a well-known medical imaging technique that utilizes computer-processed X-rays to produce tomographic images of the irradiated body part. This imaging technique is advantageous with regard to its high resolution and ease of forming a three-dimensional (3D) visual reconstruction of tissues of interest, but its inherently low sensitivity results in poor soft-tissue contrast.[146] MRI uses a very strong magnetic field and radio waves to produce images of the body, and has been a powerful imaging tool in clinical diagnosis over the past decades. T_2-weighted MRI using magnetic NPs as contrast agents exhibits high sensitivity and excellent soft-tissue contrast, but intrinsic dark signals of the contrast agents are sometimes confused with other hypointense areas, such as those resulting from air, bleeding, calcification, and metal deposition.[147] To combine MRI with CT imaging is highly desirable to overcome these limitations by combining the advantages of each modality.[148] Besides the development of diagnostic instruments, the advance of NP-based contrast agent is a prerequisite for multimodal imaging techniques.

Nowadays, the multimodal contrast agent was based on the conjugation of a CT contrast agent directly to the surface of SPION. Iodine as the most routine CT imaging agent was combined with a copolymerized monomer 2-methacryloyloxyethyl [2,3,5-triiodobenzoate] core–Fe_3O_4 satellite composite.[149] The MRI and CT test was performed in an animal model. It has been demonstrated that the as-formed composites have effects for both contrast enhancements. This study solves the problem that current embolization materials cannot be observed in imaging modalities. The optimization of embolization procedures by utilizing the complementary characteristics of MRI and CT will contribute to future improvements in embolization therapy.

Recently, a bimodality imaging agent was developed based on the conjugation of radiolabeled bisphosphonates to a magnetic particle surface.[150] CT and MR imaging studies were performed with intravenous injection of particles to a healthy six-week-old female mouse. T_2-weighted MR images of the chest and abdominal area were obtained displaying the particles rapidly accumulated in the liver and spleen. MRI results were in agreement with the CT image showing exclusive liver and spleen accumulation of radioactivity as shown in Fig. 6. This study provides a new generation of MR/CT imaging contrast agent in which the bisphosphonate group could be employed to provide targeting and radionuclides to Fe_3O_4 NPs.

As an alternative to radioactive materials, recently developed CT contrast agents such as gold NPs and tantalum oxides have also gained impetus as blood-pool X-ray contrast agents for CT.[151] Narayanan *et al.* synthesized a magnetite–gold core–satellite crystal *via* a green chemistry route using grape seed proanthocyanidin as a reducing agent.[152] The obtained Fe_3O_4–Au nanohybrids were demonstrated to have good biocompatibility, high superparamagnetism, T_2-weighted MRI contrast enhancement, and highly efficient CT contrast. They have been employed in the tracking and imaging of human mesenchymal stem cells. Li *et al.* developed multifunctional Fe_3O_4–TaOx core–shell NPs *via* the sol–gel reaction of tantalum(v) ethoxide in a microemulsion containing Fe_3O_4 NPs. This nanocomposite was proven to be biocompatible and exhibited a prolonged circulation time. The tumor-associated vessel was observed *via* MRI

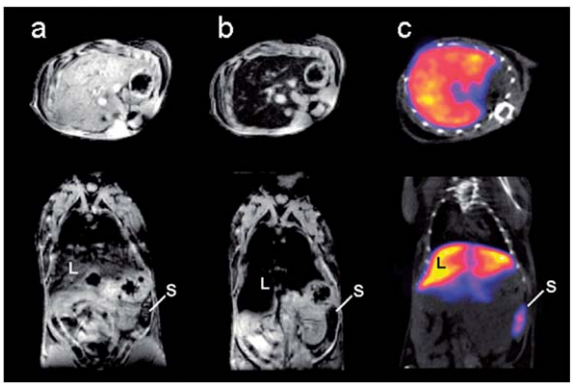

Fig. 6 Dual-modality *in vivo* studies. Short-axis view (top) and coronal view (bottom) images: (a) T_2*-weighted MR images before injection of 99mTc-DPA-ale-Endorem, (b) T_2*-weighted MR image at 15 min postinjection, and (c) nanoSPECT-CT image of the same animal in a similar view at 45 min postinjection. Contrast in the liver (L) and spleen (S) changes after injection due to accumulation of 99mTc-DPA-ale-Endorem is in agreement with the nanoSPECT-CT image which shows almost exclusive liver and spleen accumulation of radioactivity. MR images were acquired with a TE of 2 ms. Reprinted from ref. 150 with permission from the American Chemical Society.

and CT imaging after the nanocomposites were intravenously injected. The result displayed the entire vascular regions of the tumor, demonstrating that MRI shows the discrimination between the oxygenated and hypoxic regions of the tumor, whereas CT imaging reveals the tumor-associated blood vessels.

4.2 MR/optical imaging

Optical imaging displays high sensitivity, but it is limited by its high background noise from the auto-fluorescence of endogenous molecules and relatively low penetration depth in biological samples.[153] In contrast, MRI is a non-invasive imaging technique providing high-resolution 3D images of anatomic structures and physiological information about tissues *in vivo*. To bridge the gaps in resolution and sensitivity, the development of specific contrast agents for both optical and MR imaging is highly desirable.

The traditional method for making MR/optical imaging contrasts is to modify the surface of SPIONs with fluorescent molecules.[154] For instance, a SPION–RITC nanocomposite showed MR/optical bimodal imaging capability in cancer diagnosis.[155] Amine and carboxylic acid-bifunctionalized SPIONs were obtained by silanization with organofunctional alkoxysilane molecules on 25 nm SPION surfaces. A fluorophore, Rhodamine B isothiocyanate (RITC) attached onto the amine group, whereas an antibody (epithelial cell adhesion molecule-EPCAM) attached onto the carboxylic acid groups. The EPCAM antibody is specific to a protein ubiquitously expressed on the epithelial cell surface. The SPIONs–RITC was demonstrated to be able to target epithelial specific EPCAM receptors on the Panc-1pancreatic cancer cell lines. This study provides a potential effective diagnostic method and therapy for cancer aided by bimodal imaging. As an alternative to fluorescent dyes, QDs have been applied in *in vivo* imaging because most of organic dyes suffer from severe photobleaching during the detection process. A Fe_3O_4/CdTe hollow sphere has been made through the deposition of polyelectrolyte multilayers and CdTe QDs on the surface of the Fe_3O_4 hollow sphere template.[156] As-formed nanocomposite has been used as a simultaneous magnetic and optical multimodal imaging agent, and it could also be used as a controlled drug release system showing pH-sensitive drug release ability. By combining multiple functional units, the magnetic/luminescent nanocomposites are potential candidates in a variety of diagnostic techniques and therapies.

Recently, upconversion nanoparticles (UCNPs) as a new generation of optical imaging contrast agent have been extensively studied for their advantages of deep penetration, weak autofluorescence, and minimal photobleaching.[157–159] Various structured UCNPs and SPIONs have been exploited as bioimaging probes so far. They are mainly silica-modified and non-silica magnetic/upconversion nanocomposites. For instance, Lin *et al.* have developed a Fe_3O_4@nSiO_2@mSiO_2@$NaYF_4$:Yb,Er/Tm nanocomposite,[160] and Chen *et al.* synthesized a Fe_3O_4@SiO_2@Y_2O_3:Yb,Er nanocomposite,[161] both of which have a typical sandwich structure with a silica layer between the magnetic and upconversion particles. Recently, Zhang *et al.* reported a novel non-silica magnetice/upconversion Fe_3O_4@LaF_3:Yb,Er mesoparticle, which has a T_2-enhanced magnetic resonance effect and an intense visible emission under irradiation by NIR light as shown in Fig. 7.[69] The combination of magnetic NPs and UCNP will not only provide highly sensitive fluorescence imaging, but also non-invasive and high spatial resolution MR.

4.3 MR/US imaging

US, also known as diagnostic sonography, is highly cost-effective and suitable for real-time imaging ultrasound-based diagnostic imaging technique.[162,163] Although US is commonly used during pregnancy and recognized by the public, it has the limitation that the real-time imaging will be affected by bone.[164] MRI is well-known for its high quality imaging and it isn't affected by bone, while it is not real-time imaging. The integration of MRI and US should be able to give more imaging information for precise diagnosis and imaging guidance.[165]

Microbubbles or microcapsules are commonly used as US contrast agents, and they can be further functionalized with antibodies, drugs and genes to specifically bind receptors over-expressed on vascular endothelial cells.[166] Usually, the shell of a microbubble is loaded with magnetic NPs to construct a hybrid contrast agent. For instance, Liu *et al.* fabricated hybrid SPIONs-embedded poly-*n*-butylcyanoacrylate microbubbles *via* a one-pot synthesis method combining emulsion polymerization and oil-in-water encapsulation with iron oxide NPs embedded in the bubble shell.[167] For *in vivo* imaging experiments, the addition of magnetic NPs was confirmed to boost the acoustic impedance, increase back scattered signals which significantly enhanced the contrast effect of US. A similar work has also been done by

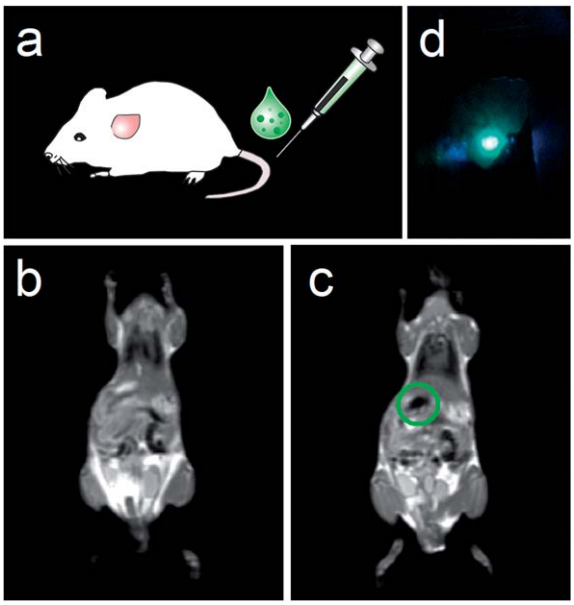

Fig. 7 (a) Schematic illustration of the Fe_3O_4@LaF_3:Yb^{3+},Er^{3+} MP solution injected into the vein tail of a mouse. T_2-weighted MR images of a mouse pre- (b) and post- (c) injection of MPs at a dose of 125 mg mL^{-1} for 30 min. The MPs are trapped in the liver and spleen. (d) Digital photograph of a frozen section of liver after 30 min injection under 980 nm laser excitation. Reproduced from ref. 69.

Yang *et al.*[168] Both of them confirmed that this kind of magnetic NPs-embedded microbubble is an interesting system for bimodal MRI/US imaging, and its enhanced contrast ratio upon US-induced destruction will enable it as a potential vehicle for drug and gene delivery.

Xu *et al.* successfully fabricated Fe_3O_4–polymer composite nanocapsules *via* a single step combine a double emulsification with the interfacial coprecipitation of iron salts.[169] The resultant nanocapsules have T_2-weighted MRI enhancement, obvious acoustic responses in an acoustic investigation, and low cytotoxicity, displaying great potential in acting as bimodal MR/US imaging contrast agents. Sun *et al.* also fabricated an organic–inorganic hybrid platform based on Fe_3O_4-containing poly(lactic-*co*-glycolicacid) microcapsules (Fe_3O_4–PLGA) for the synergistic MRI-guided high-intensity focused ultrasound liver cancer surgery.[170] Organic PLGA particles have been widely used in drug delivery and molecular imaging. By combining PLGA microcapsules with magnetic Fe_3O_4 NPs, it will enable the microcapsules with broader and more feasible applications such as MRI, magnetically targeted drug delivery and hyperthermia. Therefore, the combination of micro-bubble/capsule with SPION can facilitate both MR and US imaging-mediated transfection, gene delivery, and even broader biomedical applications.[171]

4.4 MR/PET imaging

PET imaging is a medical imaging test that uses a radioactive tracer to detect disease in the body. PET has become an essential medical tool that produces a highly sensitive 3D image or functional imaging in the body,[172,173] but it still has disadvantages with regard to spatial resolution. MR/PET bimodal imaging has great potential in clinical oncology due to its improved soft-tissue contrast and superior spatial registration compared with PET/CT imaging.[174–176] In addition to the development of multimodal imaging instruments, the nanoprobes as PET/MRI contrast agents have also been well studied over the last several years.[177]

Usually, this nanoprobe containing magnetic NPs was modified with radiometal chelators and labeled with ^{64}Cu. For instance, SPIONs were coated with 3,4-dihydroxy-D,L-phenylalanine (DL-DOPA) followed by conjugating with chelator 1,4,7,10-tetraazacyclododecane–1,4,7,10-tetraacetic acid (DOTA), which allows the chelation of ^{64}Cu for PET imaging.[178] As-prepared composites have the same cell-labeling efficacy and relaxivity as the commonly used MRI contrast agent, Feridex I.V., and have been used as dual MR/PET probes in disease detection and stem cell treatment. Nahrendorf *et al.* have made a dextranated and DTPA-modified magneto-fluorescent 20 nm NP labeled with the ^{64}Cu as a tri-modal imaging contrast agent.[179] Such an agent was directly employed in the detection of macrophages in atherosclerosis, which is the most common cause of death for the hardening of the arteries. The status of the macrophages in arteries could give information of lesion severity and therapeutic modulation. The accumulation of ^{64}Cu-SPION corresponds to macrophage burden. After intravenous injection of the agents into mice, the PET signal, combined with the MRI data, gave evidence of inflammatory plaque components. This study establishes the capability of a novel multimodality contrast agent to directly detect macrophages in atherosclerotic plaque. These studies demonstrated that MR/PET imaging will provide a better understanding of physiological and disease mechanisms in preclinical and clinical diagnosis.

5 SPIONs in therapy

SPIONs have attracted considerable interest in biomedical and clinical applications due to their unique properties such as magnetic separation, drug and gene delivery, various imaging technologies, antimicrobial, hyperthermia, and so on. This part summarizes some successful examples of multifunctional SPIONs applied in many innovative therapies.

5.1 Magnetic target gene delivery

Gene therapy is an experimental technique that uses therapeutic genes as pharmaceutical agents to treat and prevent disease.[180,181] There are two basic methods for gene delivery, namely viral vectors and non-viral vectors.[182] The main concern is the successful and intact delivery of the gene-based drugs to the exact site of disease. Taking the advantages of magnetic targeting and image contrast, SPIONs offer great potential for the efficient delivery of therapeutic genes *via* a high field magnet and monitoring the delivery process, which will open a new frontier for gene therapy in cancer treatment.[183]

In order to carry therapeutic genes into living cells, the surfaces of the magnetic particles should be modified for the attachment of target molecules using the two methods mentioned above. With respect to viral vectors, Byrne *et al.* first modified the surface of magnetic microparticles with adeno-associated virus (AAV) encoding green fluorescent protein *via* a cleavable heparin sulfate linker.[184] After intramuscular injection to mice, AAV2–SPION conjugates significantly increased the transduction efficiency in cells. Moreover, Hwang *et al.* also reported that the target efficiency has been significantly increased by modifying AAV on a heparin-coated SPION.[185] Although this delivery technology was confirmed to be useful, it may raise a lot of serious safety concerns and is not suitable for human gene therapy.

An alternative strategy for attaching DNA molecules to the particle surface is to utilize the non-viral vectors such as cationic polymers, which are capable of binding the negatively charged phosphate backbone of DNA. The most popular choice for this polymer is a branched cationic polymer polyethyleneimine (PEI).[186,187] Scherer *et al.* first employed the PEI-coated magnetic NPs for *in vitro* magnetic NP-mediated non-viral gene delivery.[186] PEI-coated SPIONs interacted with DNA *via* the electrostatic interactions and were taken up into cells by endocytosis. As a result, the magnetic controlled DNA–PEI-SPION complexes significantly reduced the duration of gene delivery and increased the transfection efficiency due to the reduced free diffusion of these particles. Shi *et al.* developed a PAH-modified Fe_3O_4@SiO_2 core/shell NP as a non-viral delivery carrier, where plasmid DNA can be easily attached.[188]

Fe_3O_4@SiO_2/PAH/DNA complex-mediated gene transfer was performed in cultured HeLa cells, and the results showed that these complexes have a high expression level but low cytotoxicity toward endothelial cells, revealing that the development of DNA technology to replace previous viral vectors paves the way for the next generation of gene therapy. In addition, Namiki *et al.* prepared an oleic acid-coated magnetite NC with a cationic lipid shell for delivering and silencing siRNA in cells and tumors in mice. This novel magnetic vector with high gene transfection efficiency and gene silencing effect could serve as a potential high-performance gene delivery system in gene therapy.[189] Recently, Medarova *et al.* developed dextran-coated SPIONs followed by modification with an NIR dye for simultaneous delivery and in *in vivo* imaging of siRNA in tumors. The delivery and silencing of the gene can be observed through MRI and optical imaging, giving a new imaging strategy for cancer therapy.[190]

5.2 Magnetic antimicrobial properties

Bacterial infection is a serious clinical problem, causing significant mortality every year.[191,192] Great effects have been devoted to developing new antibacterial drugs. However, patients with a poor immune system with prolonged exposure to anti-infective drugs became resistant to multiple antibiotics.[191] Novel strategies that combine magnetic and antibacterial properties of SPIONs and antibacterial drugs through the design of bactericide-conjugated SPIONs provide an opportunity to solve these medical problems because they can reduce the toxicity of both agents towards human cells, increase the concentration of bactericides at the action site, and facilitate interactions between bactericides and bacteria.[193,194] For instance, the cube-shaped α-Fe_2O_3 NPs with a silica shell were fabricated as substrates for the covalent immobilization and release of fluoroquinolone antibiotic sparfloxacin (SPFX).[195] SPFX-loaded NPs were demonstrated to have time-dependent release properties and low toxicity for nanomedicine applications. Another example is that antibiotic molecule (rifampicin) coated Fe_3O_4 NPs served as magnetically controllable antimicrobial agents for the recovery of bacteria loaded tissues and organs.[196] Zhang *et al.* synthesized bacitracin-conjugated Fe_3O_4 NPs by click chemistry. The bacitracin-conjugated SPIONs showed very low cytotoxicity to human fibroblast cells and exhibited a high antimicrobial efficacy against both Gram-positive and Gram-negative bacteria, which was even higher than that of bacitracin itself.[197]

In addition to antibiotics, silver (AgNPs), oxides of zinc, titanium, and copper NPs are also used in antimicrobial studies owing to their excellent antibacterial properties.[198] Among them, AgNPs with low toxicity and strong biocidal effects are the most effective antimicrobial agents against various microorganisms.[199] Targeted delivery of these AgNPs to the infectious areas can not only decrease the dose of drugs but can also achieve the controlled release of drugs. For this purpose, Prucek *et al.* synthesized Fe_3O_4@Ag and γ-Fe_2O_3@Ag NPs. These binary nanocomposites exhibited very significant antibacterial and antifungal activities against ten tested bacterial strains.[200] Zhang *et al.* developed novel hetero-Fe_3O_4–SiO_2 Janus NPs to deliver AgNPs whilst preventing their aggregation.[201] As-formed complexes have superior magnetic sensitivity, strong adhesion, and highly effective antibacterial activity, allowing us to more effectively remove and separate bacteria. Moreover, AgNPs@Fe_3O_4–SiO_2 NPs have superior biocompatibility and non-hemolytic properties, which could enhance the efficiency of sterilization in blood (Fig. 8).

A recent development in bactericidal methods is the use of photodynamic inactivation (PDI) to combat antibiotic resistant pathogenic microbes. Choi *et al.* synthesized multifunctional magnetic particles (MMPs) conjugated with a photosensititer and vancomycin.[202] Vancomycin–MMP conjugates use the non-toxic photosensitizer as a PDI agent to capture, inactivate, and remove pathogenic bacteria from the contaminated site in the presence of a magnetic field. The mechanism for PDI is that a photosensitizer can be preferentially close to the bacteria and selectively kill Gram-positive bacteria by irradiation of an appropriate wavelength to generate oxidative stress to pathogenic bacteria cell membranes. This study presented a new strategy using multifunctional PDI agents for serious bacterial contamination.

5.3 Magnetic hyperthermia

Magnetic hyperthermia is a promising adjuvant therapy for tumor treatment.[203–205] It uses multifunctional magnetic NPs to target and heat the local tumor region through Néel relaxation loss of the magnetic NPs under an external alternating magnetic field. When the temperature in tumor tissue increases to above 42–43 °C, it will induce necrotic death in cancer cells without damaging the surrounding normal tissue.

To date, a number of magnetic NPs with different functionalized surfaces were designed for thermotherapy of tumors. Jordan *et al.* exploited aminosilane- and dextran-coated SPIONs, respectively, for thermotherapy in a rat tumor model.[206] Treatments were carried out using a magnetic field applicator system. A thermotherapeutic effect was assessed by histopathological examination of the tumor tissue and the survival time of animals. The results showed that these magnetic particles are

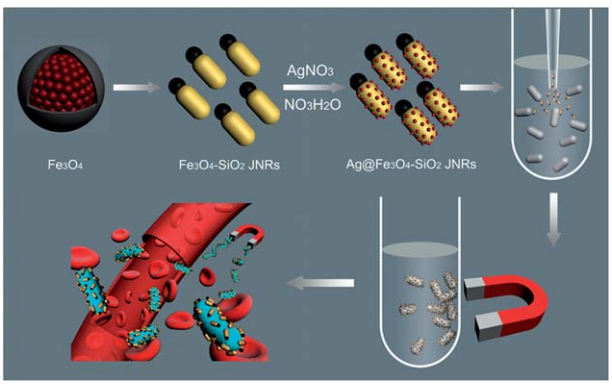

Fig. 8 Schematic illustration of a typical procedure for the *in situ* synthesis of AgNPs@Fe_3O_4–SiO_2 JNRs and their sterilization, separation process and potential antimicrobial applications in blood.

suitable for treating malignant tumors in clinical uses and aminosilane-coated particles have more advantages than the dextran-coated ones. Landeghem *et al.* also evaluated the efficacy of aminosilane-coated SPIONs in a rat model of malignant glioma.[207] The magnetic NPs were dispersed or distributed as aggregates within tumor sites of brain autopsies, displaying the uptake of NPs in glioblastoma cells. This study has confirmed the feasibility of the instillation of magnetic materials for hyperthermia in patients with glioblastoma multiforme. Fortin *et al.* developed a novel heat mediator of citrate SPIONs with uniform size and magnetic anisotropy.[208] Anionic SPIONs can serve as versatile mediators for magnetic hyperthermia in various media and appear to be good platforms for the attachment of a variety of targeting molecules. Thus, magnetic hyperthermia often combines with other therapeutic methods like radiation or chemotherapy for a synergic therapeutic effect, which will provide an increased anti-tumor effect.

Besides directly killing tumor cells, hyperthermia treatment may also cause unexpected biological responses, such as tumor-specific immune responses. Kobayashi first observed an anti-tumor immunity phenomenon by hyperthermia using magnetite NPs.[209] As shown in Fig. 9, the rats have tumors in each side of the body. Magnetic NPs were only injected into the left tumor followed by irradiation with an alternating magnetic field. After hyperthermia treatment, both left and right tumors disappeared showing an anti-tumor immune response induced by the tumor-specific hyperthermia treatment. This study demonstrated that hyperthermia not only can kill local tumors but also distant cancer cells. Recently, Cho *et al.* developed a novel magnetic switch that can turn on apoptosis cell signaling

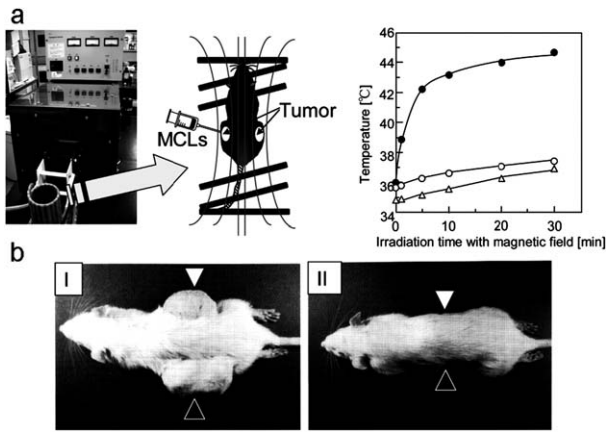

Fig. 9 Anticancer immune response induced by hyperthermia using magnetite NPs. Rats with tumors on each side of the body were prepared. (a) MCLs were injected into the left tumor only and the rats were irradiated with an alternating magnetic field using the apparatus shown (left panel). The temperature of the left tumor, containing MCLs (closed circles), increased specifically, whereas the temperature of the right tumor (open circles) and rectum (open triangles) remained below 37 °C (right panel). (b) The tumor-specific hyperthermia treatment induced an anti-tumor immune response and both tumors disappeared on the 28th day after hyperthermia treatment. (I) Control rat without AML irradiation; (II) rat with AML irradiation. Open triangle in (b), the side without MCLs; closed triangle in (b), the side with MCLs. Reprinted from ref. 209 with permission from John Wiley and Sons.

in vitro and *in vivo* under a magnetic field, which will open a new therapeutic strategy for cancer.[210]

5.4 Magnetic micro-nanomachines (MNMs)

MNMs have great promise in integrated circuits, chemical and biological sensors, and diagnosis and therapy of disease.[211–216] Great efforts have been made to develop remotely controlled MNMs, which can be guided by means of an external stimulus in narrow channels, harsh environments, and even in the human body. The recently developed MNMs are adjusted by pH or ionic strength changes, molecular fuels, and optical radiation, or thermal agitation. Promising examples are a fullerene-based MNM controlled by heat, a carborane-wheeled MNM controlled by electric field gradient, and a DNA-based MNM controlled fueled by the consumed waste of a DNA duplex.[217,218] Nevertheless, it is difficult to control the direction, time and efficiency of the motion of MNMs and is strongly restricted to the environment.

As an alternative approach, magnetically driven MNMs appear to be the most practical solution because of the low cost and simplicity of their manipulation under a magnetic field. Thanks to the development of nanotechnology, magnetic NPs as nanomachines (NMs) have been effectively exploited in the investigation of biomolecular interactions.[219] However, the basic implementation of these small magnetic NPs could not meet the need of the treatment or elimination of some medical problems such as arteriosclerosis, blood clots leading to stroke and accumulation of scar tissue. To overcome these limitations, magnetic NP-based micromachines were developed. For instance, Wang *et al.* made a 3D magnetic-controllable micromachine by electroless plating and two-photon polymerization (TPP),[220] which is a 3D micro-nanoprocessing technology for fabricating micro-nanostructures with higher spatial resolution and smaller size.[221] Tottori *et al.* reported a simple method for fabricating magnetic helical micromachines using laser writing and e-beam evaporation, which can generate a corkscrew motion with a high speed in aqueous solution and fetal bovine serum.[222] These studies would promote the development of remotely controllable MNMs from actionless micro-nanostructures to smart micro-nanorobots. However, nickel (Ni) is selected as a magnetic material in these works, which will limit their potential applications *in vivo*.

To design and fabricate a biocompatible and smart MNM for biomedical applications remains an important scientific issue. Recently, Sun and co-workers innovatively prepared a remotely controllable micro-spring of bio-compatible and degradable magnetic NPs combined with macromolecular complexes.[223] The micro-springs with excellent mechanical performance and magnetic manipulation ability were formed by TPP of a photopolymerizable resin consisting 10 nm Fe_3O_4 NPs with tightly focused femtosecond laser pulses. The motion of the spring (stretching or bending) can be controlled under a magnetic field gradient. Shortly after, they successfully fabricated a microturbine with a central axletree and three blades as shown in Fig. 10.[224–226] The rotating rate could be adjusted in the range of 0–3 r s^{-1} under a rotational magnetic field. These studies

demonstrated a novel technique for making functional MNMs with precise motion control, and gave hope for placing functional MNMs inside human blood vessels to perform disease diagnosis and treatment.

6 SPIONs in biophotonics

Biophotonics is the development and application of photonic technologies such as light sources and imaging techniques in medical, biological and life sciences research. In the previous section, conventional imaging modalities for the diagnosis and therapy of diseases at the molecular and cellular level were presented. Here, we will focus on current progresses of magnetic NP-guided optical devices and novel imaging techniques towards biomedical applications.

6.1 Photonic crystal (PC)

PCs are spatial periodic dielectric structures, which can restrict the flow of photons of selected wavelengths in an optical bandgap as semiconductors restrict the flow of electrons with energies that lie in an electronic bandgap. Besides applications in optical communication, PCs have received much attention in recent years due to its great potential in sensitive biological sensors, biomedical instrumentation and the application of laser technology in biomedicine.[227–229] For example, PCs, as an ideal encoding element of a barcode, have been used in multiple high-throughput bioassays.[230] The design and development of novel PCs will pave the way in modern therapeutic laser and photonics technologies.

As one form of PCs, colloidal photonic crystals (CPCs) have been paid considerable attention for their low lost and mass production.[231–233] Self-assembly method is considered to be the most effective and promising method for making 3D CPCs with photonic bandgaps in the near-infrared, visible or even shorter wavelength regions. The bandgaps of CPCs could be controlled by changing the refractive indices of the building blocks and the lattice constants through the application of a chemical stimulus, light or electrical fields. However, the slow response to the external stimulus limits their broad applications.

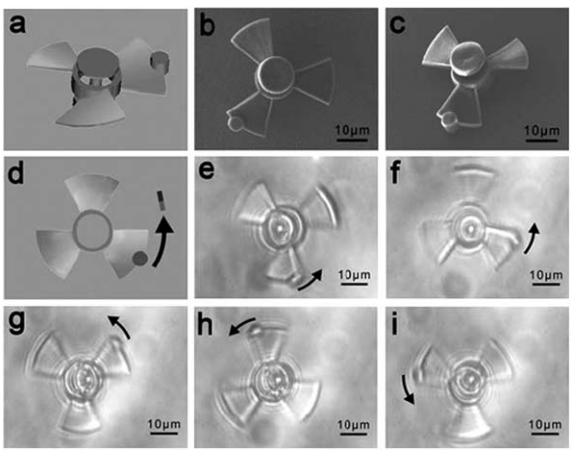

Fig. 10 Remote control of the micro-turbine in acetone. (a) Model of the micro-turbine. (b and c) SEM images of the micro-turbine. (d) Top view scheme model for circumgyratetion. (e–i) Optical microscopy images of the microturbine in a circumgyratetion cycle. For remote control and observation of the micro-turbine, a piece of ferromagnet was placed on a vortical device around the objective lens. Reprinted from ref. 224 with permission from John Wiley and Sons.

In this regard, magnetic NPs have been added to the colloidal system for the reason that the properties of CPCs could be conveniently and precisely controlled simply *via* an external magnetic field. Asher's group first developed a magnetically tunable CPC through the self-assembly of highly charged polystyrene microspheres containing magnetic NPs.[234,235] However, due to the relatively low loading of magnetic materials, the magnetic forces applied on the colloids are weaker than interparticle electrostatic forces, leading to a limited tuning range and a long response time.

Further research in increasing the magnetic response of CPC has been the fabrication of an inverse opal CPC, which can be rotated in the presence of an external magnetic field.[236] Gates *et al.* fabricated this cubic-close-packed lattice CPC by the self-assembly of monodispersed polystyrene beads in an aqueous solution containing 15 nm diameter magnetite followed by a solvent evaporation process. The filling fraction of these magnetic NPs could be conveniently changed by controlling the concentration ratio of spherical colloid-to-magnetite. An inverse opal CPC of magnetite was obtained after calcination at elevated temperatures or wet etching. Under incident light, the optical properties of such CPCs could be easily controlled by rotating the crystals with a magnet. Nevertheless, the uncontrolled formation of lattice defects in such CPCs consequently limits their practical applications.

A recent breakthrough is the work done by Yin's group, who fabricated highly charged superparamagnetic Fe_3O_4 NCs in the range of 100–180 nm.[51] These NCs can be directly employed as building blocks for the formation of magnetically tunable CPCs.[237,238] The CPCs are stabilized by the balance between the attractive magnetic force and the repulsive electrostatic force, which allow the CPCs to display various colors in the visible light region from blue to red when the strength of the applied magnetic field is decreased (Fig. 11). In addition, upon introducing a photopolymerizable resin into the above systems, the lattice structure could be easily fixed through irradiation for further study.[239] Such CPCs possess fast and fully reversible optical responses to the external magnetic field, opening the way for tunable mirrors, optical switches, and color display units.

6.2 Organic light-emitting diode (OLED)

OLEDs have attracted much attention due to their many applications in the field of lighting and flexible displaying.[240] These devices as illumination light sources could be integrated with other technologies or medical devices (such as a catheter or endoscope device) for the clinical diagnosis and treatment of disease, in which the light generated by OLEDs is received by an image sensor to produce images inside a patient's body.[241,242] However, the instability and low quantum efficiency of OLEDs is still a challenging task for its further application. Over the past two decades, significant progress in developing new materials

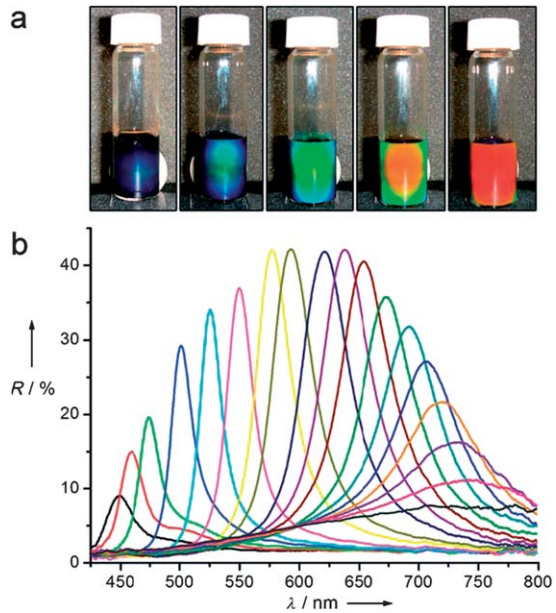

Fig. 11 (a) Images of colloidal crystals formed in response to an external magnetic field; the magnet-sample distance decreases gradually from right to left. (b) Dependence of the reflection spectra at normal incidence of the colloidal crystals on the distance of the sample from the magnet. Diffraction peaks blue-shift (from right to left) as the distance decreases from 3.7 to 2.0 cm with step sizes of 0.1 cm. Reprinted from ref. 237 with permission from John Wiley and Sons.

and light extraction concepts has been made for the improvement of brightness and efficiency of OLEDs. Here, the use of a magnetite electrode in OLEDs was simply introduced.

Sun's group have systematically studied employing Fe_3O_4 NPs as an electrode modification layer and p type dopant to significantly enhance the luminance efficiency of OLEDs due to the unique properties of Fe_3O_4 NPs, such as low-cost, non-toxicity, high spin polarization, high Curie temperature, and low electrical resistivity at room temperature.[243–247] In their early work, Fe_3O_4 NPs were inserted between an indium tin oxide (ITO) anode and the emitting layer of *N*,*N*′-diphenyl-*N*,*N*′-bis-(1-naphthyl)-(1,1′-biphenyl)-4,4′-diamine (NPB) as an electrode modification layer and p type dopant.[245] The luminance of OLEDs has been effectively enhanced through the reduction of the energy barrier at the ITO/Fe_3O_4/NPB interface and the improvement of the hole injection/transport property by introduction of magnetic NPs. Furthermore, they investigated the magnetic field effect on the OLEDs with SPIONs. Fe_3O_4 NPs have been respectively applied to OLEDs as an efficient anodic buffer and magnetic dopant. Under an external magnetic field, 10.5% enhancement of current efficiency for the Fe_3O_4 buffered OLEDs has been observed compared to that without the magnetic field.[244] The enhancement can be explained by the increase of the singlet exciton fraction due to the hole spin polarization injection. As magnetic dopants, Fe_3O_4 NPs were used in the hole-transport layer of OLEDs to increase the ratio of hole spin polarization. An enhancement of 24% for the current efficiency was obtained, which has a linear dependence on the magnetic field intensity.[247] These studies demonstrated that the use of Fe_3O_4 in OLEDs can give an efficient pathway to enhance the performance of OLEDs. The design and fabrication of novel OLEDs with low cost, high brightness and efficiency, and chemical stability is still a major trend of OLED technology for biomedical imaging and lighting applications.

6.3 Magnetic particle imaging (MPI)

Since MPI was first reported by Gleich and Weizenecker in 2005, it has generated widespread attention in medicine and material science.[248] MPI technique exploits the non-linear response property of iron oxide NPs to localize their spatial position, which is a potential 3D real-time imaging of NP contrast agent at spatial resolutions.[249] MPI is also a safe imaging technique compared to CT and PET imaging which use radioactive materials as contrast agents. This novel tomographic imaging technique is designed around magnetic NPs rather than developing a contrast agent to work with an existing imaging technique.[250] MPI has the potential to be state of the art in clinically adopted imaging modality.

The optimal sensitivity and resolution will occur for monodisperse SPIONs with large size and high saturation magnetization. However, larger NPs will influence the magneto-viscous relaxation resulting in a lower signal of the contrast agent. Although a study has reported that a 30 nm SPION will generate better MPI images, the optimization of magnetic NPs is still to be studied.[251] In addition to the contrast agent, MPI scanning as a powerful and exciting area of research to improve sensitivity and improved spatial resolution of MPI has been paid great attention.[252] MPI scanners are based upon a setup consisting of two selection and drive field coils, two drive field coils and signal receive coils, as shown in Fig. 12a, in which the resulting 2D field-of-view is obtained in between the coils. For instance, Weizenecker *et al.* have succeeded in employing MPI to image SPIONs flowing through the cardiovascular system of a living mouse with high temporal and spatial resolution.[253] It can generate sensitive signals by using a commercial MRI contrast agent (Resovist, the second clinically approved SPION-based MRI tracer) at clinically tolerable dosages. Another promising work has been reported by Goodwill *et al.*[251] By using this two-sided MPI scanner, small animal images were acquired showing the distribution of SPIONs in a mouse. As shown in Fig. 12c, the MPI imaging of the mouse was acquired 30 s after tail vein injection with 20 μL (556 μg Fe) of Resovist, after which the SPION has arrived at the brain, heart, and liver. In contrast, the SPIONs were concentrated in the liver 5 min after injection, displaying the capability of MPI for *in vivo* 3D high-resolution real-time imaging (Fig. 12d). From the MPI images, it can be concluded that MPI has a superior contrast effect compared to MRI and a higher resolution than optical imaging.

In this two-sided scanner, the size limitation of the object being imaged means that the object should be situated in between the coils. Researchers aimed to create a setup in the same way as a US transducer in which all coils are positioned on one side of the patient (Fig. 12b). In this regard, a single-sided MPI scanner has been developed and used for experimental cancer detection of the sentinel lymph node biopsy.[254] Despite

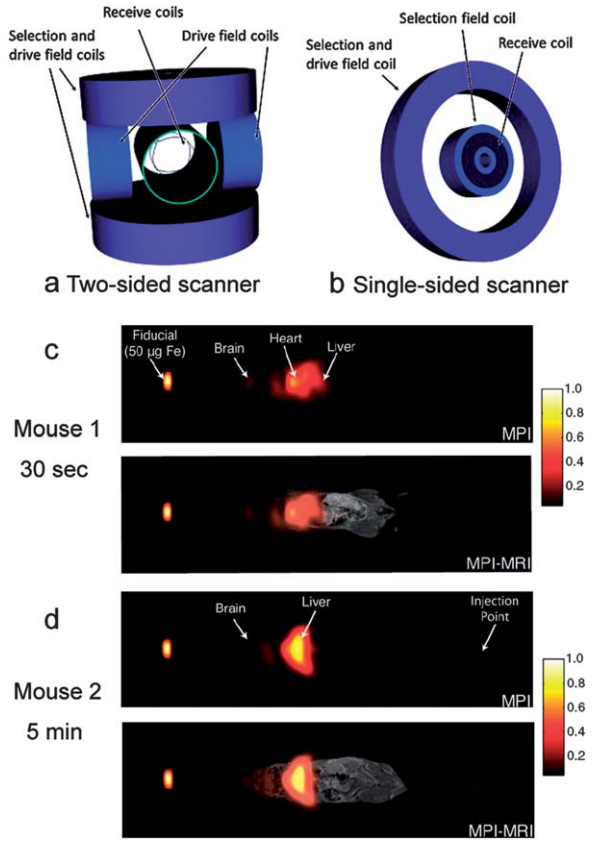

Fig. 12 Schematic drawing of different MPI scanner topologies: an MPI scanner where the field of view lies in the center of a two-sided scanner (a), and a single-sided MPI scanner (b) where all coils lie on one side of the field of view. (c) Full-body MPI projection scan of a mouse injected in the tail vein with 20 µL (556 µg Fe) undiluted Resovist tracer and sacrificed after 30 s (c) and 5 minutes (d). The resulting MPI image shows an MPI-MRI visible fiducial (50 µg Fe, scaled to signal value of 1.0), as well as the outlines of the mouse brain, heart, and liver. Reprinted from ref. 251 with permission from John Wiley and Sons.

technological innovations, only dynamic 2D MPI images could been obtained currently, motivating researchers for the optimization of the tracer and scanner of MPI for clinically adopted imaging modality.

7 Conclusion and perspective

In this review, we outline the recent advances in multifunctional SPIONs for biomedical photonic applications. Various common chemistry concepts have been applied in the design and synthesis of two kinds of SPIONs: core/shell- and hetero-structured particles. These uniquely structured particles not only promise biomedical applications in genes, viruses, tumor cells, early detection, *etc.* but also, as new classes of contrast agents and photonic probes, they offer advantages for bio-photonic applications into the investigation and therapy of genetic diseases, viral infections, cancer and various other diseases. Besides, SPIONs open up a new avenue to novel optical devices and imaging techniques.

Although these developments are encouraging, considerable challenges and issues still need to be resolved. First, it is necessary to design novel types of multifunctional SPIONs with precise composition, superior performance of each functional unit, and controlled surface modification. Methods for large-scale production are demanding to achieve commercial and clinical applications. The structural and physical properties between different units is rarely studied and therefore needs to be investigated for determining the stability and utility of the whole composite. Secondly, it is crucial to study in detail the biocompatibility, biodistribution, long-term stability, and toxicological effect from the perspective of safe use of these multifunctional composites. Particularly, the interaction of SPIONs with biological systems needs to be well studied before they begin to be used in humans, and their targeting capabilities *in vivo* need to be enhanced. Lastly, the size and magnetic properties of SPIONs are still to be optimized for the development of magnetic NPs-based light sources and imaging technique. Despite these numerous challenges, SPIONs are indeed promising for highly sensitive diagnostic, excellent multimodal imaging, efficient therapeutic and novel photonic applications.

Acknowledgements

HBS thanks the supported by the National Science Foundation of China (Grant no. 90923037) and the National Basic Research program of China (973 Program) (Grant no. 2011CB013005). WFD thanks the financial support from the National Science Foundation of China (Grant nos 91123029, 61077066, 61137001 and 61127010).

Notes and references

1 R. Hao, R. J. Xing, Z. C. Xu, Y. L. Hou, S. Gao and S. H. Sun, *Adv. Mater.*, 2010, **22**, 2729.
2 I. Brigger, C. Dubernet and P. Couvreur, *Adv. Drug Delivery Rev.*, 2002, **54**, 631.
3 C. Sun, K. Du, C. Fang, N. Bhattarai, O. Veiseh, F. Kievit, Z. Stephen, D. Lee, R. G. Ellenbogen, B. Ratner and M. Zhang, *ACS Nano*, 2010, **4**, 2402.
4 A. Ito, M. Shinkai, H. Honda and T. Kobayashi, *J. Biosci. Bioeng.*, 2005, **100**, 1.
5 J. H. Gao, H. W. Gu and B. Xu, *Acc. Chem. Res.*, 2009, **42**, 1097.
6 M. Mahmoudi, S. Sant, B. Wang, S. Laurent and T. Sen, *Adv. Drug Delivery Rev.*, 2011, **63**, 24.
7 A. K. Gupta and M. Gupta, *Biomaterials*, 2005, **26**, 3995.
8 F. Sonvico, C. Dubernet, P. Colombo and P. Couvreur, *Curr. Pharm. Des.*, 2005, **11**, 2091.
9 J. Dobson, *Drug Dev. Res.*, 2006, **67**, 55.
10 L. A. Thomas, L. Dekker, M. Kallumadil, P. Southern, M. Wilson, S. P. Nair, Q. A. Pankhurstand and I. P. Parkin, *J. Mater. Chem.*, 2009, **19**, 6529.
11 A. Jordan, R. Scholz, K. Maier-Hauff, F. K. H. van Landeghem, N. Waldoefner, U. Teichgraeber, J. Pinkernelle, H. Bruhn, F. Neumann, B. Thiesen, A. von Deimling and R. Felix, *J. Neuro-Oncol.*, 2006, **78**, 7.
12 E. S. Day, J. G. Morton and J. L. West, *J. Biomech. Eng.*, 2009, **131**, 074001.

13 Q. Zhang, J. Ge, J. Goebl, Y. Hu, Y. Sun and Y. Yin, *Adv. Mater.*, 2010, **22**, 1905.
14 W. Zhao, J. Gu, L. Zhang, H. Chen and J. Shi, *J. Am. Chem. Soc.*, 2005, **127**, 8916.
15 Z. Xu, Y. Hou and S. Sun, *J. Am. Chem. Soc.*, 2007, **129**, 8698.
16 W. Schartl, *Nanoscale*, 2010, **2**, 829.
17 S. Y. Wei, Q. Wang, J. H. Zhu, L. Y. Sun, H. F. Lin and Z. H. Gu, *Nanoscale*, 2011, **3**, 4474.
18 P. P. Yang, S. L. Gai and J. Lin, *Chem. Soc. Rev.*, 2012, **41**, 3679.
19 A. K. Salem, P. C. Searson and K. W. Leong, *Nat. Mater.*, 2003, **2**, 668.
20 D. Graham-Rowe, *Nat. Photonics*, 2007, **1**, 248.
21 S. C. Glotzer and M. J. Solomon, *Nat. Mater.*, 2007, **6**, 557.
22 J. V. Herrikhuyzen, G. Portale, J. C. Gielen, P. C. M. Christianen, N. A. J. M. Sommerdijk, S. C. J. Meskers and A. P. H. J. Schenning, *Chem. Commun.*, 2008, 697.
23 S. Laurent, D. Forge, M. Port, A. Roch, C. Robic, L. V. Elst and R. N. Muller, *Chem. Rev.*, 2008, **108**, 2064.
24 T. Hyeon, *Chem. Commun.*, 2003, 927.
25 Y. Deng, L. Wang, W. Yang, S. Fu and A. Elaissari, *J. Magn. Magn. Mater.*, 2003, **257**, 69.
26 T. Hyeon, S. S. Lee, J. Park, Y. Chung and H. B. Na, *J. Am. Chem. Soc.*, 2001, **123**, 12798.
27 R. Abu Mukh-Qasem and A. Gedanken, *J. Colloid Interface Sci.*, 2005, **284**, 489.
28 C. C. Berry and A. S. G. Curtis, *J. Phys. D: Appl. Phys.*, 2003, **36**, R198.
29 N. A. Frey, S. Peng, K. Cheng and S. H. Sun, *Chem. Soc. Rev.*, 2009, **38**, 2532.
30 R. Fu, X. M. Jin, J. L. Liang, W. S. Zheng, J. Q. Zhuang and W. S. Yang, *J. Mater. Chem.*, 2011, **21**, 15352.
31 M. Hu, J. Y. Chen, Z. Y. Li, L. Au, G. V. Hartland, X. D. Li, M. Marquez and Y. N. Xia, *Chem. Soc. Rev.*, 2006, **35**, 1084.
32 X. Michalet, F. F. Pinaud, L. A. Bentolila, J. M. Tsay, S. Doose, J. J. Li, G. Sundaresan, A. M. Wu, S. S. Gambhir and S. Weiss, *Science*, 2005, **307**, 538.
33 J. Shen, L. D. Sun, Y. W. Zhang and C. H. Yan, *Chem. Commun.*, 2010, **46**, 5731.
34 S. T. Selvan, P. K. Patra, C. Y. Ang and J. Y. Ying, *Angew. Chem., Int. Ed.*, 2007, **46**, 2448.
35 B. H. Wu, H. Zhang, C. Chen, S. C. Lin and N. F. Zheng, *Nano Res.*, 2009, **2**, 975.
36 S. Santra, H. S. Yang, P. H. Holloway, J. T. Stanley and R. A. Mericle, *J. Am. Chem. Soc.*, 2005, **127**, 1656.
37 S. Mornet, S. Vasseur, F. Grasset and E. Duguet, *J. Mater. Chem.*, 2004, **14**, 2161.
38 C. Sun, J. S. H. Lee and M. Zhang, *Adv. Drug Delivery Rev.*, 2008, **60**, 1252.
39 J. P. Jolivet, C. Chaneac and E. Tronc, *Chem. Commun.*, 2004, 481.
40 Y. S. Kang, S. Risbud, J. F. Rabolt and P. Stroeve, *Chem. Mater.*, 1996, **8**, 2209.
41 J. Park, K. J. An, Y. S. Hwang, J. G. Park, H. J. Noh, J. Y. Kim, J. H. Park, N. M. Hwang and T. Hyeon, *Nat. Mater.*, 2004, **3**, 891.
42 S. G. Kwon, Y. Piao, J. Park, S. Angappane, Y. Jo, N. M. Hwang, J. G. Park and T. Hyeon, *J. Am. Chem. Soc.*, 2007, **129**, 12571.
43 S. Sun and H. Zeng, *J. Am. Chem. Soc.*, 2002, **124**, 8204.
44 Y. Hou, Z. Xu and S. Sun, *Angew. Chem., Int. Ed.*, 2007, **46**, 6329.
45 T. Hyeon, S. Seong Lee, J. Park, Y. Chung and H. B. Na, *J. Am. Chem. Soc.*, 2001, **123**, 12798.
46 H. Deng, X. L. Li, Q. Peng, X. Wang, J. P. Chen and Y. D. Li, *Angew. Chem., Int. Ed.*, 2005, **44**, 2782.
47 S. B. Wang, Y. L. Min and S. H. Yu, *J. Phys. Chem. C*, 2007, **111**, 3551.
48 S. Agarwala, Z. H. Lim, E. Nicholson and G. W. Ho, *Nanoscale*, 2012, **4**, 194.
49 Y. L. Hou, J. F. Yu and S. Gao, *J. Mater. Chem.*, 2003, **13**, 1983.
50 J. Wang, M. Yao, G. J. Xu, P. Cui and J. T. Zhao, *Mater. Chem. Phys.*, 2009, **113**, 6.
51 J. P. Ge, Y. X. Hu, M. Biasini, W. P. Beyermann and Y. D. Yin, *Angew. Chem., Int. Ed.*, 2007, **46**, 4342.
52 Z. G. Teng, X. G. Zhu, G. F. Zheng, F. Zhang, Y. H. Deng, L. C. Xiu, W. Li, Q. Yang and D. Y. Zhao, *J. Mater. Chem.*, 2012, **22**, 17677.
53 K. A. Morch, *Phys. Fluids*, 2007, **19**, 072104.
54 K. Tachibana and S. Tachibana, *Echocardiography*, 2001, **18**, 323.
55 K. S. Suslick and S. J. Doktycz, *Adv. Sonochem.*, 1990, **1**, 197.
56 J. H. Bang and K. S. Suslick, *J. Am. Chem. Soc.*, 2007, **129**, 2242.
57 W. Stöber, A. Fink and E. Bohn, *J. Colloid Interface Sci.*, 1968, **26**, 62.
58 H. L. Ding, Y. X. Zhang, S. Wang, J. M. Xu, S. C. Xu and G. H. Li, *Chem. Mater.*, 2012, **24**, 4572.
59 Y. Lu, Y. D. Yin, B. T. Mayers and Y. N. Xia, *Nano Lett.*, 2002, **2**, 183.
60 T. L. Fare, E. M. Coffey, H. Y. Dai, Y. D. D. He, D. A. Kessler, K. A. Kilian, J. E. Koch, L. P. Eric, M. J. Marton, M. R. Meyer, R. B. Stoughton, G. Y. Tokiwa and Y. Q. Wang, *Anal. Chem.*, 2003, **75**, 4672.
61 X. H. Gao and S. M. Nie, *Anal. Chem.*, 2004, **76**, 2406.
62 D. S. Wang, J. B. He, N. Rosenzweig and Z. Rosenzweig, *Nano Lett.*, 2004, **4**, 409.
63 L. L. Li, H. B. Li, D. Chen, H. Y. Liu, F. Q. Tang, Y. Q. Zhang, J. Ren and Y. Li, *J. Nanosci. Nanotechnol.*, 2009, **9**, 2540.
64 G. F. Wang, Q. Peng and Y. D. Li, *Acc. Chem. Res.*, 2011, **44**, 322.
65 G. Mialon, S. Türkcan, G. Dantelle, D. P. Collins, M. Hadjipanayi, R. A. Taylor, T. Gacoin, A. Alexandrou and J. P. Boilot, *J. Phys. Chem. C*, 2010, **114**, 22449.
66 Y. P. Li, J. H. Zhang, X. Zhang, Y. S. Luo, X. G. Ren, H. F. Zhao, X. J. Wang, L. D. Sun and C. H. Yan, *J. Phys. Chem. C*, 2009, **113**, 4413.
67 Z. Y. Ma, D. Dosev, M. Nichkova, S. J. Gee, B. D. Hammock and I. M. Kennedy, *J. Mater. Chem.*, 2009, **19**, 4695.
68 J. Zhou, Z. Liu and F. Y. Li, *Chem. Soc. Rev.*, 2012, **41**, 1323.
69 L. Zhang, Y. S. Wang, Y. Yang, F. Zhang, W. F. Dong, S. Y. Zhou and H. B. Sun, *Chem. Commun.*, 2012, **48**, 11238.

70 Z. Xu, Y. Hou and S. Sun, *J. Am. Chem. Soc.*, 2007, **129**, 8698.
71 B. Chudasama, A. K. Vala, N. Andhariya, R. V. Upadhyay and R. V. Mehta, *Nano Res.*, 2009, **2**, 955.
72 L. Zhang, W. F. Dong, Z. Y. Tang, J. F. Song, H. Xia and H. B. Sun, *Opt. Lett.*, 2010, **35**, 3297.
73 J. Yan, M. Bloom, S. C. Bae, E. Luijten and S. Granick, *Nature*, 2012, **491**, 578.
74 S. C. Glotzer and M. J. Solomon, *Nat. Mater.*, 2007, **6**, 557.
75 Y. D. Jin and X. H. Gao, *Nat. Nanotechnol.*, 2009, **4**, 571.
76 T. Mokari, E. Rothenberg, I. Popov, R. Costi and U. Banin, *Science*, 2004, **304**, 1787.
77 D. Graham-Rowe, *Nat. Photonics*, 2007, **1**, 248.
78 A. K. Salem, P. C. Searson and K. W. Leong, *Nat. Mater.*, 2003, **2**, 668.
79 H. Yu, M. Chen, P. M. Rice, S. X. Wang, R. L. White and S. Sun, *Nano Lett.*, 2005, **5**, 379.
80 C. Wang, H. Daimon and S. Sun, *Nano Lett.*, 2009, **9**, 1493.
81 L. Zhang, Y. H. Dou and H. C. Gu, *J. Colloid Interface Sci.*, 2006, **297**, 660.
82 Y. Pan, J. H. Gao, B. Zhang, X. X. Zhang and B. Xu, *Langmuir*, 2010, **26**, 4184.
83 N. Zhao and M. Y. Gao, *Adv. Mater.*, 2009, **21**, 184.
84 L. Zhang, F. Zhang, W. F. Dong, J. F. Song, Q. S. Huo and H. B. Sun, *Chem. Commun.*, 2011, **47**, 1225.
85 L. Zhang, F. Zhang, Y. S. Wang, Y. L. Sun, W. F. Dong, J. F. Song, Q. S. Huo and H. B. Sun, *Soft Matter*, 2011, **7**, 7375.
86 M. Feyen, C. Weidenthaler, F. Schuthand and A. Lu, *J. Am. Chem. Soc.*, 2010, **132**, 6791.
87 K. W. Kwon and M. Shim, *J. Am. Chem. Soc.*, 2005, **127**, 10269.
88 N. R. Jana, Y. F. Chen and X. G. Peng, *Chem. Mater.*, 2004, **16**, 3931.
89 S. H. Kim, S. J. Jeon, W. C. Jeong, H. S. Park and S. M. Yang, *Adv. Mater.*, 2008, **20**, 1.
90 L. Y. Wang, J. W. Bai, Y. J. Li and Y. Huang, *Angew. Chem., Int. Ed.*, 2008, **47**, 2439.
91 S. H. Xuan, Y. X. J. Wang, J. C. Yu and K. C. F. Leung, *Langmuir*, 2009, **25**, 11835.
92 K. C. F. Leung, S. H. Xuan, X. M. Zhu, D. W. Wang, C. P. Chak, S. F. Lee, W. K. W. Ho and B. C. T. Chung, *Chem. Soc. Rev.*, 2012, **41**, 1911.
93 S. R. Wang, J. Zhang, X. H. Liu, X. Z. Guo and S. H. Wu, *Chem.–Eur. J.*, 2010, **16**, 8108.
94 Y. Wang, Y. H. Shen, A. J. Xie, S. K. Li, X. F. Wang and Y. Cai, *J. Phys. Chem. C*, 2010, **114**, 4297.
95 H. L. Zhu, E. Zhu, G. F. Ou, L. H. Gao and J. J. Chen, *Nanoscale Res. Lett.*, 2010, **5**, 1755.
96 K. M. Yeo, S. I. Lee, Y. T. Lee, Y. K. Chung and I. S. Lee, *Chem. Lett.*, 2008, **37**, 116.
97 J. H. Lee, Y. W. Jun, S. I. Yeon, J. S. Shin and J. Cheon, *Angew. Chem., Int. Ed.*, 2006, **45**, 8160.
98 O. Veiseh, C. Sun, J. Gunn, N. Kohler, P. Gabikian, D. Lee, N. Bhattarai, R. Ellenbogen, R. Sze, A. Hallahan, J. Olson and M. Q. Zhang, *Nano Lett.*, 2005, **5**, 1003.
99 R. N. Mitra, M. Doshi, X. L. Zhang, J. C. Tyus, N. Bengtsson, S. Fletcher, B. D. G. Page, J. Turkson, A. J. Gesquiere, P. T. Gunning, G. A. Walter and S. Santraa, *Biomaterials*, 2012, **33**, 1500.
100 X. Hong, J. Li, M. J. Wang, J. J. Xu, W. Guo, J. H. Li, Y. B. Bai and T. J. Li, *Chem. Mater.*, 2004, **16**, 4022.
101 V. Wagner, A. Dullaart, A. K. Bock and A. Zweck, *Nat. Biotechnol.*, 2006, **24**, 1211.
102 M. E. Davis, Z. Chen and D. M. Shin, *Nat. Rev. Drug Discovery*, 2008, **7**, 771.
103 D. S. Millar, S. J. Withey, M. L. V. Tizard, J. G. Ford and J. Hermon-Taylor, *Anal. Biochem.*, 1995, **226**, 325.
104 C. C. Chou, C. H. Chen, T. T. Lee and K. Peck, *Nucleic Acids Res.*, 2004, **32**, e99.
105 O. Olsvik, T. Popovic, E. Skjerve, K. S. Cudjoe, E. Hornes, J. Ugelstad and M. Uhlen, *Clin. Microbiol. Rev.*, 1994, **7**, 43.
106 A. Jungell-Nortamo, A. C. Syvänen, P. Luoma and H. Söderlund, *Mol. Cell. Probes*, 1988, **2**, 281.
107 N. J. Parham, F. J. Picard, R. Peytavi, M. Gagnon, G. Seyrig, P. A. Gagne, M. Boissinot and M. G. Bergeron, *Clin. Chem.*, 2007, **53**, 1570.
108 D. Xi, X. P. Luo, Q. H. Lu, K. L. Yao, Z. L. Liu and Q. Ning, *J. Nanopart. Res.*, 2008, **10**, 393.
109 S. F. Kingsmore, *Nat. Rev. Drug Discovery*, 2006, **5**, 310.
110 T. I. Williams, K. L. Toups, D. A. Saggese, K. R. Kalli, W. A. Cliby and D. C. Muddiman, *J. Proteome Res.*, 2007, **6**, 2936.
111 P. R. Nair and M. A. Alam, *Analyst*, 2010, **135**, 2798.
112 J. M. Nam, C. S. Thaxton and C. A. Mirkin, *Science*, 2003, **301**, 1884.
113 J. M. Perez, L. Josephson, T. O'Loughlin, D. Högemann and R. Weissleder, *Nat. Biotechnol.*, 2002, **20**, 816.
114 H. Lee, E. Sun, D. Ham and R. Weissleder, *Nat. Med.*, 2008, **14**, 869.
115 H. L. Shao, C. W. Min, D. Lssador, M. Liong, T. J. Yoon, R. Weissleder and H. Lee, *Theranostics*, 2012, **2**, 55.
116 J. B. Haun, C. M. Castro, R. Wang, V. M. Peterson, B. S. Marinelli, H. Lee and R. Weissleder, *Sci. Transl. Med.*, 2011, **3**, 71ra16.
117 R. S. Gaster, L. Xu, S. J. Han, R. J. Wilson, D. A. Hall, S. J. Osterfeld, H. Yu and S. X. Wang, *Nat. Nanotechnol.*, 2011, **6**, 314.
118 S. J. Osterfeld, H. Yu, R. S. Gaster, S. Caramuta, L. Xu, S. J. Han, D. A. Hall, R. J. Wilson, S. H. Sun, R. L. White, R. W. Davis, N. Pourmand and S. X. Wang, *Proc. Natl. Acad. Sci. U. S. A.*, 2008, **105**, 52.
119 R. S. Gaster, D. A. Hall, G. H. Nielsen, S. J. Osterfeld, H. Yu, K. E. Mach, R. J. Wilson, B. Murmann, J. C. Liao, S. S. Gambhir and S. X. Wang, *Nat. Med.*, 2009, **15**, 1327.
120 M. V. Yigit, D. Mazumdar and Y. Lu, *Bioconjugate Chem.*, 2008, **19**, 412.
121 L. H. Liu, H. Dietsch, P. Schurtenberger and M. Yan, *Bioconjugate Chem.*, 2009, **20**, 1349.
122 K. Ikuta, M. S. Ibrahim, T. Kobayashi and K. Tomonaga, *Front. Biosci.*, 2002, **7**, 470.
123 T. Jartti, M. Söderlund-Venermo, K. Hedman, O. Ruuskanen and M. J. Makela, *Paediatr. Respir. Rev.*, 2013, **14**, 38.

124 Y. Amano and Q. Cheng, *Anal. Bioanal. Chem.*, 2005, **381**, 156.
125 A. Sakudo, K. Baba, M. Tsukamoto and K. Ikuta, *Bioorg. Med. Chem. Lett.*, 2009, **19**, 4488.
126 T. L. Kamikawa, M. G. Mikolajczyk, M. Kennedy, P. Zhang, W. Wang, D. E. Scott and E. C. Alocilja, *Biosens. Bioelectron.*, 2010, **26**, 1346.
127 E. L. Munson, D. J. Diekema, S. E. Beekmann, K. C. Chapin and G. V. Doern, *J. Clin. Microbiol.*, 2003, **41**, 495.
128 N. Sanvicens, C. Pastells, N. Pascual and M. P. Marco, *TrAC, Trends Anal. Chem.*, 2009, **28**, 1243.
129 C. Corot, P. Robert, J. M. Idee and M. Port, *Adv. Drug Delivery Rev.*, 2006, **58**, 1471.
130 H. L. Grossman, W. R. Myers, V. J. Vreel, R. Bruehl, M. D. Alper, C. R. Bertozzi and J. Clarke, *Proc. Natl. Acad. Sci. U. S. A.*, 2004, **101**, 129.
131 K. El-Boubbou, C. Gruden and X. Huang, *J. Am. Chem. Soc.*, 2007, **129**, 13392.
132 M. Koets, T. vander Wijk, J. T. W. M. van Eemeren, A. van Amerongen and M. W. J. Prins, *Biosens. Bioelectron.*, 2009, **24**, 1893.
133 P. A. Suci, D. L. Berglund, L. Liepold, S. Brumfield, B. Pitts, W. Davison, L. Oltrogge, K. O. Hoyt, S. Codd, P. S. Stewart, M. Young and T. Douglas, *Chem. Biol.*, 2007, **14**, 387.
134 J. H. Lee, Y. M. Huh, Y. W. Jun, J. W. Seo, J. T. Jang, H. T. Song, S. J. Kim, E. J. Cho, H. G. Yoon, J. S. Suh and J. W. Cheon, *Nat. Med.*, 2006, **13**, 95.
135 D. C. Dorn, U. Harnack and G. Pecher, *Anticancer Res.*, 2004, **24**, 821.
136 C. Tang, P. J. Russell, R. Martiniello-Wilks, J. E. J. Rasko and A. Khatri, *Stem Cells*, 2010, **28**, 1686.
137 X. Wu, J. Hu, L. F. Zhou, Y. Mao, B. Yang, L. Gao, R. Xie, F. Xu, D. Zhang, J. Liu and J. H. Zhu, *J. Neurosurg.*, 2008, **108**, 320.
138 H. Choi, S. R. Choi, R. Zhou, H. F. Kung and I. W. Chen, *Acad. Radiol.*, 2004, **11**, 996.
139 T. J. Chen, T. H. Cheng, Y. C. Hung, K. T. Lin, G. C. Liu and Y. M. Wang, *J. Biomed. Mater. Res., Part A*, 2008, **87A**, 165.
140 M. K. Yu, J. Park, Y. Y. Jeong, W. K. Moon and S. Jon, *Nanotechnology*, 2010, **21**, 415102.
141 A. Toma, E. Otsuji, Y. Kuriu, K. Okamoto, D. Ichikawa, A. Hagiwara, H. Ito, T. Nishimura and H. Yamagishi, *Br. J. Cancer*, 2005, **93**, 131.
142 T. Suwa, S. Ozawa, M. Ueda, N. Ando and M. Kitajima, *Int. J. Cancer*, 1998, **75**, 626.
143 J. E. Smith, C. D. Medley, Z. Tang, D. Shangguan, C. Lofton and W. Tan, *Anal. Chem.*, 2007, **79**, 3075.
144 J. K. Herr, J. E. Smith, C. D. Medley, D. H. Shangguan and W. H. Tan, *Anal. Chem.*, 2006, **78**, 2918.
145 M. V. Yigit, D. Mazumdar, H. K. Kim, J. H. Lee, B. Odintsov and Y. Lu, *ChemBioChem*, 2007, **8**, 1675.
146 I. Hernandez-Giron, J. Geleijns, A. Calzado and W. J. H. Veldkamp, *Med. Phys.*, 2011, **38**, S25.
147 H. B. Na, I. C. Song and T. Hyeon, *Adv. Mater.*, 2009, **21**, 2133.
148 J. Gao, H. Gu and B. Xu, *Acc. Chem. Res.*, 2009, **42**, 1097.
149 S. H. Bartling, J. Budjan, H. Aviv, S. Haneder, B. Kraenzlin, H. Michaely, S. Margel, S. Diehl, W. Semmler, N. Gretz, S. O. Schönberg and M. Sadick, *Invest. Radiol.*, 2011, **46**, 178.
150 R. T. Martin de Rosales, R. Tavare, A. Glaria, G. Varma, A. Protti and P. J. Blower, *Bioconjugate Chem.*, 2011, **22**, 455.
151 N. Lee, H. R. Cho, M. H. Oh, S. H. Lee, K. Kim, B. H. Kim, K. Shin, T. Y. Ahn, J. W. Choi, Y. W. Kim, S. H. Choi and T. Hyeon, *J. Am. Chem. Soc.*, 2012, **134**, 10309.
152 S. Narayanan, B. N. Sathy, U. Mony, M. Koyakutty, S. V. Nair and D. Menon, *ACS Appl. Mater. Interfaces*, 2012, **4**, 251.
153 L. Q. Xiong, Z. G. Chen, Q. W. Tian, T. Y. Cao, C. J. Xu and F. Y. Li, *Anal. Chem.*, 2009, **81**, 8687.
154 G. Lamanna, M. Kueny-Stotz, H. Mamlouk-Chaouachi, C. Ghobril, B. Basly, A. Bertin, I. Miladi, C. Billotey, G. Pourroy, S. Begin-Colin and D. Felder-Flesch, *Biomaterials*, 2011, **32**, 8562.
155 C. I. Olariu, H. H. P. Yiu, L. Bouffier, T. Nedjadi, E. Costello, S. R. Williams, C. M. Halloran and M. J. Rosseinsky, *J. Mater. Chem.*, 2011, **21**, 12650.
156 L. Li, H. Li, D. Chen, H. Liu, F. Tang, Y. Zhang, J. Ren and Y. Li, *J. Nanosci. Nanotechnol.*, 2009, **9**, 2540.
157 F. Wang, Y. Han, C. S. Lim, Y. H. Lu, J. Wang, J. Xu, H. Y. Chen, C. Zhang, M. H. Hong and X. G. Liu, *Nature*, 2010, **463**, 1061.
158 A. Xia, Y. Gao, J. Zhou, C. Y. Li, T. S. Yang, D. M. Wu, L. M. Wu and F. Y. Li, *Biomaterials*, 2011, **32**, 7200.
159 X. Zhu, J. Zhou, M. Chen, M. Shi, W. Feng and F. Li, *Biomaterials*, 2012, **33**, 4618.
160 S. L. Gai, P. P. Yang, C. X. Li, W. X. Wang, Y. L. Dai, N. Niu and J. Lin, *Adv. Funct. Mater.*, 2010, **20**, 1166.
161 X. G. Yu, Y. Shan, G. C. Li and K. Z. Chen, *J. Mater. Chem.*, 2011, **21**, 8104.
162 M. Grass, R. Koppe, E. Klotz, R. Proksa, M. H. Kuhn, H. Aerts, J. Op de Beek and R. Kemkers, *Comput. Med. Imaging Graphics*, 1999, **23**, 311.
163 S. J. Norton and T. Vo-Dinh, *IEEE Trans. Med. Imaging*, 2007, **26**, 660.
164 A. Brounstein, I. Hacihaliloglu, P. Guy, A. Hodgson and R. Abugharbieh, *Med. Image Comput. Comput. Assist Interv.*, 2011, **14**, 235.
165 M. Viallon, S. Terraz, J. Roland, E. Dumont, C. D. Becker and R. Salomir, *Med. Phys.*, 2010, **37**, 1491.
166 J. Oh, M. D. Feldman, J. Kim, C. Condit, S. Emelianov and T. E. Milner, *Nanotechnology*, 2006, **17**, 4183.
167 Z. Liu, T. Lammers, J. Ehling, S. Fokong, J. Bornemann, F. Kiessling and J. Gätjens, *Biomaterials*, 2011, **32**, 6155.
168 F. Yang, Y. Li, Z. Chen, Y. Zhang, J. Wu and N. Gu, *Biomaterials*, 2009, **30**, 3882.
169 B. Xu, H. Dou, K. Tao, K. Sun, J. Ding, W. Shi, X. Guo, J. Li, D. Zhang and K. Sun, *Langmuir*, 2011, **27**, 12134.
170 Y. Sun, Y. Zheng, H. Ran, Y. Zhou, H. Shen, Y. Chen, H. Chen, T. M. Krupka, A. Li, P. Li, Z. Wang and Z. Wang, *Biomaterials*, 2012, **33**, 5854.
171 B. Sharma, A. Martin and I. Zerizer, *Seminars in Ultrasound, CT and MRI*, 2013, **34**, 66.
172 W. M. Xu, M. Feng, H. Y. Zhao, M. X. Xie, W. Y. Li and R. Fu, *J. Huazhong Univ. Sci. Technol., Med. Sci.*, 2013, **33**, 146.

173 F. F. Chao and H. Zhang, *J. Biomed. Biotechnol.*, 2012, 783739.
174 J. Lee, S. Lee, S. J. Kim, J. W. Choi and K. W. Baek, *Dentomaxillofacial Radiology*, 2013, **42**, 29292350.
175 B. Aklan, D. H. Paulus, E. Wenkel, H. Braun, B. K. Navalpakkam, S. Ziegler, C. Geppert, E. E. Sigmund, A. Melsaether and H. H. Quick, *Med. Phys.*, 2013, **40**, 024301.
176 H. Zaidi and A. D. Guerra, *Med. Phys.*, 2011, **38**, 5667.
177 J. Choi, J. C. Park, H. Nah, S. Woo, J. Oh, K. M. Kim, G. J. Cheon, Y. M. Chang, J. S. Yoo and J. W. Cheon, *Angew. Chem., Int. Ed.*, 2008, **47**, 6259.
178 D. Patel, A. Kell, B. Simard, B. Xiang, H. Y. Lin and G. H. Tian, *Biomaterials*, 2011, **32**, 1167.
179 M. Nahrendorf, H. Zhang, S. Hembrador, P. Panizzi, D. E. Sosnovik, E. Aikawa, P. Libby, F. K. Swirski and R. Weissleder, *Circulation*, 2008, **117**, 379.
180 H. Mok, O. Veiseh, C. Fang, F. M. Kievit, F. Y. Wang, J. O. Park and M. Zhang, *Mol. Pharmaceutics*, 2010, **7**, 1930.
181 F. M. Kievit, O. Veiseh, C. Fang, N. Bhattarai, D. Lee, R. G. Ellenbogen and M. Zhang, *ACS Nano*, 2010, **4**, 4587.
182 F. M. Kievit and M. Q. Zhang, *Acc. Chem. Res.*, 2011, **22**, 853.
183 F. M. Kievit, O. Veiseh, N. Bhattarai, C. Fang, J. W. Gunn, D. Lee, R. G. Ellenbogen, J. M. Olson and M. Zhang, *Adv. Funct. Mater.*, 2009, **19**, 2244.
184 C. Mah, I. Zolotukhin, T. J. Fraites, J. Dobson, C. Batich and B. J. Byrne, *Mol. Ther.*, 2000, **1**, S239.
185 J. H. Hwang, S. Lee, E. Kim, J. S. Kim, C. H. Lee, I. S. Ahn and J. H. Jang, *Int. J. Pharm.*, 2011, **421**, 397.
186 F. Scherer, M. Anton, U. Schillinger, J. Henke, C. Bergemann, A. Krüger, B. Gänsbacher and C. Plank, *Gene Ther.*, 2002, **9**, 102.
187 R. Namgung, K. Singha, M. K. Yu, S. Jon, Y. S. Kim, Y. Ahn, I. K. Park and W. J. Kim, *Biomaterials*, 2010, **31**, 4204.
188 M. R. Shi, Y. Y. Liu, M. M. Xu, H. Yang, C. H. Wu and H. Miyoshi, *Macromol. Biosci.*, 2011, **11**, 1563.
189 Z. Medarova, W. Pham, C. Farrar, V. Petkova and A. Moore, *Nat. Med.*, 2007, **13**, 372.
190 Y. Namiki, T. Namiki, H. Yoshida, Y. Ishii, A. Tsubota, S. Koido, K. Nariai, M. Mitsunaga, S. Yanagisawa, H. Kashiwagi, Y. Mabashi, Y. Yumoto, S. Hoshina, K. Fujise and N. Tada, *Nat. Nanotechnol.*, 2009, **4**, 598.
191 A. G. Mainous, V. A. Diaz, E. M. Matheson, S. H. Gregorie and W. J. Hueston, *Public Health Rep.*, 2011, **126**, 354.
192 C. S. Zinn, H. Westh and V. T. Rosdahl, *Microb. Drug Resist.*, 2004, **10**, 160.
193 V. Nizet, T. Ohtake, X. Lauth, J. Trowbridge, J. Rudisill, R. A. Dorschner, V. Pestonjamasp, J. Piraino, K. Huttner and R. L. Gallo, *Nature*, 2001, **414**, 454.
194 P. Li, J. Li, C. Wu, Q. Wu and J. Li, *Nanotechnology*, 2005, **16**, 1912.
195 N. E. A. El-Gamel, L. Wortmann, K. Arroub and S. Mathur, *Chem. Commun.*, 2011, **47**, 10076.
196 C. Nădejde, E. F. Ciurlică, D. Creangă, A. Cârlescu and V. Bădescu, *AIP Conf. Proc.*, 2010, **1311**, 388.
197 W. J. Zhang, X. H. Shi, J. Huang, Y. X. Zhang, Z. R. Wu and Y. Z. Xian, *ChemPhysChem*, 2012, **13**, 3388.
198 V. Thati, A. S. Roy, M. V. N. Ambika Prasad, C. T. Shivannavar and S. M. Gaddad, *J. Biosci. Tech.*, 2010, **1**, 64.
199 C. N. Lok, C. M. Ho, R. Chen, Q. Y. He, W. Y. Yu, H. Sun, P. K. Tam, J. F. Chiu and C. M. Che, *JBIC, J. Biol. Inorg. Chem.*, 2007, **12**, 527.
200 R. Prucek, J. Tuček, M. Kilianová, A. Panáček, L. Kvítek, J. Filip, M. Kolář, K. Tománková and R. Zbořil, *Biomaterials*, 2011, **32**, 4704.
201 L. Zhang, Q. Luo, F. Zhang, D. M. Zhang, Y. S. Wang, Y. L. Sun, W. F. Dong, J. Q. Liu, Q. S. Huo and H. B. Sun, *J. Mater. Chem.*, 2012, **22**, 23741.
202 K. H. Choi, H. J. Lee, B. J. Park, K. K. Wang, E. P. Shin, J. C. Park, Y. K. Kim, M. K. Oh and Y. R. Kim, *Chem. Commun.*, 2012, **48**, 4591.
203 R. Hergt and S. Dutz, *J. Magn. Magn. Mater.*, 2007, **311**, 187.
204 M. Johannsen, U. Gneveckow, L. Eckelt, A. Feussner, N. Waldofner, R. Scholz, S. Deger, P. Wust, S. A. Loening and A. Jordan, *Int. J. Hyperthermia*, 2005, **21**, 637.
205 J. P. Fortin, C. Wilhelm, J. Servais, C. Menager, J. C. Bacri and F. Gazeau, *J. Am. Chem. Soc.*, 2007, **129**, 2628.
206 A. Jordan, R. Scholz, K. Maier-Hauff, F. K. van Landeghem, N. Waldoefner, U. Teichgraeber, J. Pinkernelle, H. Bruhn, F. Neumann, B. Thiesen, A. von Deimling and R. Felix, *J. Neuro-Oncol.*, 2006, **78**, 7.
207 F. K. van Landeghem, K. Maier-Hauff, A. Jordan, K. T. Hoffmann, U. Gneveckow, R. Scholz, B. Thiesen, W. Brück and A. von Deimling, *Biomaterials*, 2009, **30**, 52.
208 J. Fortin, C. Wilhelm, J. Servais, C. Ménager, J. Bacri and F. Gazeau, *J. Am. Chem. Soc.*, 2007, **129**, 2628.
209 T. Kobayashi, *Biotechnol. J.*, 2011, **6**, 1342.
210 M. H. Cho, E. J. Lee, M. Son, J. H. Lee, D. W. Yoo, J. W. Kim, S. W. Park, J. S. Shin and J. W. Cheon, *Nat. Mater.*, 2012, **11**, 1038.
211 M. D. Dickey, K. J. Russell, D. J. Lipomi, V. Narayanamurti and G. M. Whitesides, *Small*, 2010, **6**, 2050.
212 Y. Q. Fu, H. J. Du, W. M. Huang, S. Zhang and M. Hu, *Sens. Actuators, A*, 2004, **112**, 395.
213 A. C. R. Grayson, R. S. Shawgo, A. M. Johnson, N. T. Flynn, Y. W. Li, M. J. Cima and R. Langer, *Proc. IEEE*, 2004, **92**, 6.
214 M. Y. Gao, C. Z. Hu, Z. Z. Chen, S. Liu and H. H. Zhang, *IEEE Trans. Biomed. Eng.*, 2009, **56**, 2413.
215 K. Ishiyama, M. Sendoh and K. I. Arai, *J. Magn. Magn. Mater.*, 2002, **41**, 242.
216 Y. Shirai, A. J. Osgood, Y. Zhao, Y. Yao, L. Saudan, H. Yang, C. Y. Hung, L. B. Alemany, T. Sasaki, J. F. Morin, J. M. Guerrero, K. F. Kelly and J. M. Tour, *J. Am. Chem. Soc.*, 2006, **128**, 4854.
217 T. Sasaki and J. M. Tour, *Tetrahedron Lett.*, 2007, **48**, 5821.
218 T. Omabegho, R. Sha and N. C. Seeman, *Science*, 2009, **324**, 67.
219 I. De Vlaminck and C. Dekker, *Annu. Rev. Biophys.*, 2012, **41**, 453.
220 W. K. Wang, Z. B. Sun, M. L. Zheng, X. Z. Dong, Z. S. Zhao and X. M. Duan, *J. Phys. Chem. C*, 2011, **115**, 11275.
221 W. Xiong, Y. S. Zhou, X. N. He, Y. Gao, M. Mahjouri-Samani, L. Jiang, T. Baldacchini and Y. F. Lu, *Light: Sci. Appl.*, 2012, **1**, e6.

222 S. Tottori, L. Zhang, F. Qiu, K. K. Krawczyk, A. Franco-Obregón and B. J. Nelson, *Adv. Mater.*, 2012, **24**, 811.
223 J. Wang, H. Xia, B. B. Xu, L. G. Niu, D. Wu, Q. D. Chen and H. B. Sun, *Opt. Lett.*, 2009, **34**, 581.
224 H. Xia, J. Wang, Y. Tian, Q. D. Chen, X. B. Du, Y. L. Zhang, Y. He and H. B. Sun, *Adv. Mater.*, 2010, **22**, 3204.
225 Y. Tian, Y. L. Zhang, H. Xia, L. Guo, J. F. Ku, Y. He, R. Zhang, B. Z. Xu, Q. D. Chen and H. B. Sun, *Phys. Chem. Chem. Phys.*, 2011, **13**, 4835.
226 Y. Tian, Y. L. Zhang, J. F. Ku, Y. He, B. B. Xu, Q. D. Chen, H. Xia and H. B. Sun, *Lab Chip*, 2010, **10**, 2902.
227 E. Yablonovitch, *Phys. Rev. Lett.*, 1987, **58**, 2059.
228 S. John, *Phys. Rev. Lett.*, 1987, **58**, 2486.
229 Y. Akahane, T. Asano, B. S. Song and S. Noda, *Nature*, 2003, **425**, 944.
230 Y. J. Zhao, Z. Y. Xie, H. C. Gu, L. Jin, X. W. Zhao, B. P. Wang and Z. Z. Gu, *NPG Asia Mater.*, 2012, **4**, e25.
231 W. L. Vos, R. Sprik, A. vanBlaaderen, A. Imhof, A. Lagendijk and G. H. Wegdam, *Phys. Rev. B: Condens. Matter*, 1996, **53**, 16231.
232 R. C. Schroden, M. Al-Daous, C. F. Blanford and A. Stein, *Chem. Mater.*, 2002, **14**, 3305.
233 J. M. Weissman, H. B. Sunkara, A. S. Tse and S. A. Asher, *Science*, 1996, **274**, 959.
234 X. Xu, G. Friedman, K. D. Humfeld, S. A. Majetich and S. A. Asher, *Chem. Mater.*, 2002, **14**, 1249.
235 X. Xu, G. Friedman, K. D. Humfeld, S. A. Majetich and S. A. Asher, *Adv. Mater.*, 2001, **13**, 1681.
236 B. Gates and Y. N. Xia, *Adv. Mater.*, 2001, **13**, 1605.
237 J. Ge, Y. Hu, M. Biasini, W. P. Beyermann and Y. Yin, *Angew. Chem.*, 2007, **119**, 4420.
238 J. P. Ge and Y. D. Yin, *J. Mater. Chem.*, 2008, **18**, 5041.
239 H. Xia, L. Zhang, Q. D. Chen, L. Guo, H. H. Fang, X. B. Li, J. F. Song, X. R. Huang and H. B. Sun, *J. Phys. Chem. C*, 2009, **113**, 18542.
240 A. Köhler, J. S. Wilson and R. H. Friend, *Adv. Mater.*, 2002, **14**, 701.
241 P. Rai, P. S. Kumar and V. K. Varadan, *Proc. SPIE–Int. Soc. Opt. Eng.*, 2010, **7646**, 76460Z.
242 M. Scholles, L. Kroker, U. Vogel, J. Krüger, R. Walczak and J. Ruano-Lopez, *Proc. SPIE–Int. Soc. Opt. Eng.*, 2010, **7593**, 75930C.
243 D. D. Zhang, J. Feng, Y. Q. Zhong, Y. F. Liu, H. Wang, Y. Jin, Y. Bai, Q. D. Chen and H. B. Sun, *Org. Electron.*, 2010, **11**, 1891.
244 J. Feng, D. D. Zhang, Y. F. Liu, Y. Bai, Q. D. Chen, S. Y. Liu and H. B. Sun, *J. Phys. Chem. C*, 2010, **114**, 6718.
245 D. D. Zhang, J. Feng, Y. F. Liu, Y. Q. Zhong, Y. Bai, Y. Jin, G. H. Xie, Q. Xue, Y. Zhao, S. Y. Liu and H. B. Sun, *Appl. Phys. Lett.*, 2004, **94**, 223306.
246 D. D. Zhang, J. Feng, L. Chen, H. Wang, Y. F. Liu, Y. Jin, Y. Bai, Y. Q. Zhong and H. B. Sun, *IEEE J. Quantum Electron.*, 2011, **47**, 591.
247 D. D. Zhang, J. Feng, H. Wang, Y. F. Liu, L. Chen, Y. Jin, Y. Q. Zhong, Y. Bai, Q. D. Chen and H. B. Sun, *IEEE Photonics J.*, 2011, **3**, 26.
248 B. Gleich and J. Weizenecker, *Nature*, 2005, **435**, 1214.
249 P. W. Goodwill, A. Tamrazian, L. R. Croft, C. D. Lu, E. M. Johnson, R. Pidaparthi, R. M. Ferguson, A. P. Khandhar, K. M. Krishnan and S. M. Conolly, *Appl. Phys. Lett.*, 2011, **98**, 262502.
250 B. Gleich, J. Weizenecker and J. Borgert, *Phys. Med. Biol.*, 2008, **53**, N81.
251 P. W. Goodwill, E. U. Saritas, L. R. Croft, T. N. Kim, K. M. Krishnan, D. V. Schaffer and S. M. Conolly, *Adv. Mater.*, 2012, **24**, 3870.
252 T. F. Sattel, T. Knopp, S. Biederer, B. Gleich, J. Weizenecker, J. Borgert and T. M. Buzug, *J. Phys. D: Appl. Phys.*, 2009, **42**, 1.
253 J. Weizenecker, B. Gleich, J. Rahmer, H. Dahnke and J. Borgert, *Phys. Med. Biol.*, 2009, **54**, L1.
254 B. Ruhland, K. Baumann, T. Knopp, T. Sattel, S. Biederer, K. Luedtke-Buzug, T. M. Buzug, K. Diedrich and D. Finas, *Geburtshilfe und Frauenheilkunde*, 2009, **69**, 758.

